

AD-A162 778

STUDY OF CHARACTERISTICS OF DRY FRICTION DAMPING(U)  
UNITED TECHNOLOGIES RESEARCH CENTER EAST HARTFORD CT  
A V SRINIVASAN ET AL MAR 84 UTRC/R84-956479-1

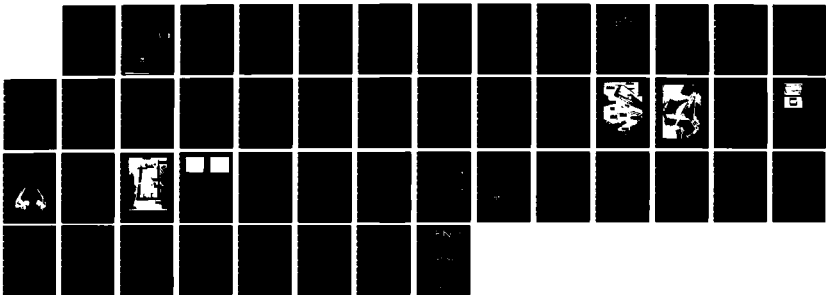
**1/1**

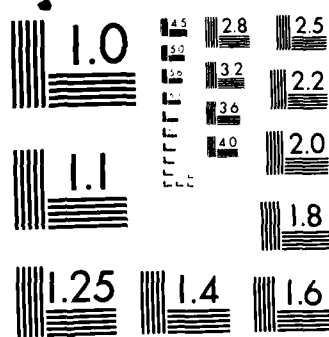
UNCLASSIFIED

AFOSR-TR-85-1074 F49620-83-C-0076

**F/G 28/11**

NL





MICROCOPY RESOLUTION TEST CHART  
NATIONAL BUREAU OF STANDARDS 1963-A

# STUDY OF CHARACTERISTICS OF DRY FRICTION DAMPING

A.V.Srinivasan  
B.N.Cassenti  
D.G.Cutts

ANNUAL REPORT  
March 1984

DTIC  
ELECTE  
DEC 30 1985  
S D

AD-A162 770

Prepared for

AIR FORCE OFFICE OF SCIENTIFIC RESEARCH  
Bolling AFB, Washington, DC 20332

CONTRACT F49620-83-C-0076

DTIC FILE COPY



UNITED  
TECHNOLOGIES  
RESEARCH  
CENTER

East Hartford, Connecticut 06108

Approved for public release;  
distribution unlimited.

85 12 30 036

Unclassified

SECURITY CLASSIFICATION OF THIS PAGE (When Data Entered):

| REPORT DOCUMENTATION PAGE  |   | READ INSTRUCTIONS<br>BEFORE COMPLETING FORM   |
|--|---|---|
| 1. REPORT NUMBER<br><b>AFOSR-TR- 85-1074</b><br><del>R84-956479-1</del>  | 2. GOVT ACCESSION NO.<br><b>AD-A161 170</b> | 3. RECIPIENT'S CATALOG NUMBER   |
| 4. TITLE (and Subtitle)<br>Study of Characteristics of Dry Friction Damping  |   | 5. TYPE OF REPORT & PERIOD COVERED<br>Annual Technical Report                                       |
| 7. AUTHOR(s)<br>A. V. Srinivasan, B. N. Cassenti, and D. G. Cutts  |   | 6. PERFORMING ORG. REPORT NUMBER<br>R84-956479-1  |
| 9. PERFORMING ORGANIZATION NAME AND ADDRESS<br>United Technologies Corporation<br>United Technologies Research Center<br>Silver Lane, East Hartford, CT 06108  |   | 8. CONTRACT OR GRANT NUMBER(s)<br>F49620-83-C-0076  |
| 11. CONTROLLING OFFICE NAME AND ADDRESS<br>AFOSR/NA USAF/AFSC<br>Directorate of Aerospace Sciences<br>Bldg 410, Bolling Air Force Base, DC 20332   |   | 10. PROGRAM ELEMENT, PROJECT, TASK AREA & WORK UNIT NUMBERS<br><b>61102F</b><br>Project No. 2307/B1 |
| 14. MONITORING AGENCY NAME & ADDRESS (if different from Controlling Office)<br>Air Force Plant Representative Office<br>Det 5, Pratt & Whitney Aircraft Group<br>400 Main Street<br>East Hartford, CT 06108 Code FY1725  |   | 12. REPORT DATE<br>March 1984   |
|  |   | 13. NUMBER OF PAGES<br>45   |
| 16. DISTRIBUTION STATEMENT (of this Report)<br><br><del>none</del><br><br>Approved for public release;<br>distribution unlimited.  |   | 15. SECURITY CLASS. (of this report)<br>Unclassified  |
| 17. DISTRIBUTION STATEMENT (of the abstract entered in Block 20, if different from Report)<br><br>none   |   | 15a. DECLASSIFICATION DOWNGRADING SCHEDULE  |
| 18. SUPPLEMENTARY NOTES<br><br>none  |   |   |
| 19. KEY WORDS (Continue on reverse side if necessary and identify by block number)<br><br>Dry Friction<br>Damping<br>Vibrations<br>Structural Dynamics   |   |   |
| 20. ABSTRACT (Continue on reverse side if necessary and identify by block number)<br><br>This report pertains to the overall problem of estimating damping due to dry friction forces induced at interfaces of vibrating components. The phase of the effect reported here contains the summary of a literature survey and identifies the scope of research needed.<br><br>The survey clearly indicated the complex processes involved during rubbing of one component relative to another bringing into |   |   |

DD FORM 1 JAN 73 1473

EDITION OF 1 NOV 65 IS OBSOLETE

SECURITY CLASSIFICATION OF THIS PAGE (When Data Entered):

Unclassified

SECURITY CLASSIFICATION OF THIS PAGE(When Data Entered)

play a host of parameters. Very limited data, especially of a fundamental nature, appears to be available in regard to dry friction in a vibratory environment.

An analytical and corresponding experimental plan is presented and discussed. These plans include (a) considerations of new laws of friction appropriate to vibration analyses and (b) corresponding basic experiments from which a data base can be developed for use in design of structural components.

The principal contents of this report were presented in the form of a paper entitled "Characteristics of Dry Friction Damping", at the Air Force sponsored Vibration Damping Workshop held in Long Beach, California, February 27-29, 1984.

This annual report covers the period between March 1, 1983 and March 1, 1984. The work reported herein was under sponsorship of the AFOSR under the technical direction of Dr. A. Amos.

Unclassified

SECURITY CLASSIFICATION OF THIS PAGE(When Data Entered)

R84-956479-1

STUDY OF CHARACTERISTICS OF DRY FRICTION DAMPING

TABLE OF CONTENTS

|   | <u>Page</u> |
|---|-------------|
| SUMMARY . . . . .   | i           |
| 1.0 INTRODUCTION . . . . .  | 1           |
| 2.0 REVIEW OF THE LITERATURE . . . . .  | 3           |
| 2.1 Interface Characteristics . . . . .   | 3           |
| 2.2 Characterization of Friction Forces . . . . .                                     | 8           |
| 2.2.1 Coefficient of Friction . . . . .   | 17          |
| 2.3 Dry Friction Damping Technology . . . . .   | 20          |
| 3.0 RESEARCH ISSUES AND PLANS . . . . .   | 26          |
| REFERENCES  |             |
| APPENDIX A - SINGLE DEGREE OF FREEDOM MODEL . . . . .                                 | 36          |
| APPENDIX B - APPLICATION OF FINITE ELEMENT CODES TO<br>DRY FRICTION DAMPING . . . . . | 41          |

AIR FORCE OVERSEAS OPERATIONAL  
NOTICE OF  
CHIEF OF  
MAY 1984  
CHIEF OF

## SUMMARY

This report pertains to the overall problem of estimating damping due to dry friction forces induced at interfaces of vibrating components. The phase of the effort reported here contains the summary of a literature survey and identifies the scope of research needed.

The survey clearly indicated the complex processes involved during rubbing of one component relative to another bringing into play a host of parameters. Very limited data, especially of a fundamental nature, appears to be available in regard to dry friction in a vibratory environment.

An analytical and corresponding experimental plan is presented and discussed. These plans include (a) considerations of new laws of friction appropriate to vibration analyses and (b) corresponding basic experiments from which a data base can be developed for use in design of structural components.

The principal contents of this report were presented in the form of a paper entitled "Characteristics of Dry Friction Damping", at the Air Force sponsored Vibration Damping Workshop, held in Long Beach, California, February 27-29, 1984.

This annual report covers the period between March 1, 1983 and March 1, 1984. The work reported herein was under sponsorship of the AFOSR under the technical direction of Dr. A. Amos.

|                    |                                     |
|--------------------|-------------------------------------|
| Accession For      |                                     |
| NTIS               | <input checked="" type="checkbox"/> |
| CRA&I              | <input type="checkbox"/>            |
| DTIC               | <input type="checkbox"/>            |
| TAB                | <input type="checkbox"/>            |
| Unannounced        | <input type="checkbox"/>            |
| Justification      |                                     |
| By                 |                                     |
| Distribution/      |                                     |
| Availability Codes |                                     |
| Dist               | Avail and/or<br>Special             |
| A-1                |                                     |



## 1. INTRODUCTION

The structural integrity of engineering systems depends to a large extent on the levels of energy dissipation that can occur when the system is subjected to time dependent forces. One of the most important sources of energy dissipation in built-up structures pertains to dry friction at joints and at interfaces in contact with each other. When materials with very low inherent damping are used in environments offering essentially no aerodynamic damping (such as, for example, in space structural systems), the ability of the structures to withstand resonant vibration depends almost entirely on the extent of friction damping. Even in the design of components which can generate certain levels of aerodynamic damping, it is essential to be able to estimate accurately the levels of non-aerodynamic sources of damping because unlike the latter, the former can be either positive or negative. For example, the aeroelastic instabilities of aircraft structures such as airplane wings or turbomachinery blades are attributed to negative aerodynamic damping developing in the system as a result of its interaction with the air forces causing the system to vibrate. In such situations, escalation of vibratory stresses to dangerous levels is prevented only through the contribution to damping from sources such as friction. In some instances, artificial devices are designed and introduced into the structural system with the sole purpose of developing friction forces leading to damping when the dynamics of the component demands it. Thus, there is a clear need to enhance the level of understanding in the broad area of dynamics of surfaces in contact.

Friction between contacting interfaces which undergo relative vibratory motion is known to dissipate the energy of vibration resulting in damped oscillations. The phenomenon of friction between contacting surfaces is probably the most elusive physical mechanism that defies clear comprehension. The complexity of the phenomenon of friction damping arises from the variations in the type of time dependent motions developing at an interface. These variations in the relative motion at the contacting surfaces span the extremes between microslip and gross motion and include local slip, stick-slip motion, chatter, etc. The parameters that control the resulting motion include the normal forces holding the surfaces together, their distribution, properties of materials in contact, surface treatments, temperature, frequency of vibration, level of vacuum, coefficient of dynamic friction, etc. The phenomenon is clearly nonlinear and the feasibility of linearization needs to be established.

In the context of vibration engineering, the basic requirements are to (a) quantify the nature and magnitude of friction forces that are manifest between contacting interfaces of vibrating components, (b) quantify the nature and magnitude of vibratory motion at these interfaces, and (c) predict the



extent of damping that may be present. Within this context, friction forces are considered to be useful, i.e. they control vibratory amplitudes which otherwise may escalate. On the other hand, any consideration of friction forces cannot ignore the influence of these forces on wear of the components resulting in loss of useful life of machines. The phenomena of friction and wear are thus inseparable. The emphasis in this study, however, is in outlining those aspects of friction forces that pertain to vibration damping.

## 2. REVIEW OF THE LITERATURE

In order to assess the state-of-the-art in the area of damping due to dry friction, a literature search was initiated. It became clear that the subject matter could be classified into at least three specialized disciplines comprising efforts in the areas of (a) surface science (b) characterization of friction forces at mating surfaces and (c) damping technology. Further, there appears to be very limited data, especially of a fundamental nature, obtained in a vibratory environment in which friction forces play a significant role. The developments in each of these areas have occurred somewhat independent of each other because each represents an area important in itself providing considerable research opportunities. Future developments must, however, attempt to integrate these efforts in order to be able to obtain accurate and reliable estimates of energy dissipation in vibrating systems.

An excellent treatment of the science of friction and wear is found in a book Friction and Wear: Calculation Methods (Ref. 1) by the Russian authors Kragelsky, Dobychin and Komalov. The chapter on "Dry and Boundary Friction" should be of special interest to researchers in this field and has an excellent treatment of the subject beginning as far back as 1508 when Leonardo da Vinci established the simple law of friction which assumed the friction force to be proportional to the normal load. Researchers should also find the three volumes of the book on Friction, Wear, Lubrication (Ref. 2) edited by Kragelsky and Alisin. Another book, also by Russian authors Panovko and Gubanova entitled Stability and Oscillation of Elastic Systems (Ref. 3) treats the subject of self-induced oscillations with dry friction. In addition, the proceedings volume of a NASA-sponsored symposium on Interdisciplinary Approach to Friction and Wear (Ref. 4) edited by Ku contains material which covers the several aspects of surface topography, friction, and adhesion, wear, etc. These books along with the papers that will be referred to in the sections below have served as the basis for the viewpoints presented in this report. Because of the interdisciplinary nature of the subject matter, no claim will be made that all the relevant literature has been surveyed here. The reader may, therefore, draw to the authors' attention relevant books or papers not included in this preliminary survey so that a more complete list of references may emerge at the end of this research effort.

### 2.1 Interface Characteristics

Surfaces of real components used in engineering practice are never ideally smooth so that when they come into contact with each other, the contact cannot be continuous and only certain parts of the surface will carry the applied load (see Fig. 1). Thus, the true contact area is the sum of those parts of the surfaces where the interaction between the bodies is strong. The true contact area is the result of penetration or crushing of individual asperities, and, therefore, the contact area increases with

increasing deformation. The real contact area is much smaller than the apparent area of contact and can be as low as ".01 to .1% of the apparent contact area" (see Ref. 2).

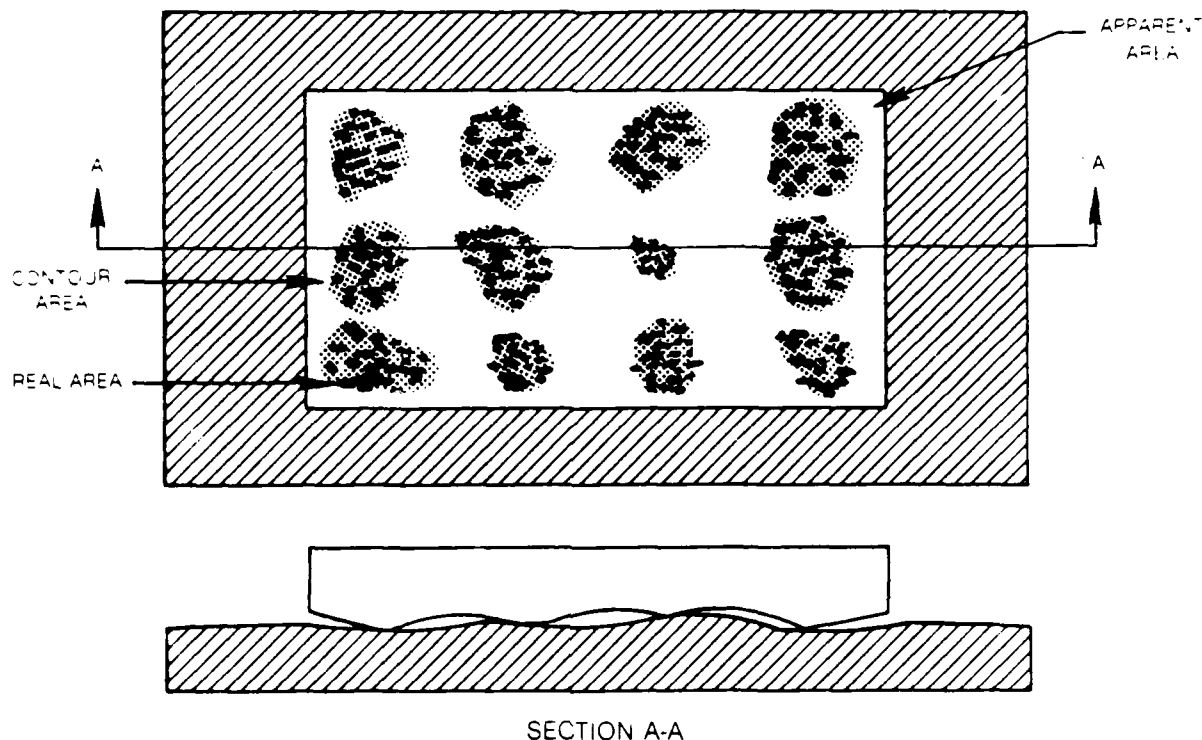


Figure 1. Contact Areas

The research pertaining to the mechanism governing the formation of true contact area goes back to 1939 when Bowden and Tabor (Ref. 5) determined, on the basis of measurement of electrical conductivity, that the true contact area changes in direct proportion to the normal load  $N$ . In elastic contact, this was shown to be  $A \approx N^{2/3}$ . Further generalization for practical application in all cases of contact between metallic surfaces led to the relationship  $A = N/\sigma_y$ , where  $\sigma_y$  = yield stress of the soft material. This law is considered to be applicable only when the tips of spherical asperities lie at the same level.

V. A. Zhuravlev, (Ref. 6) whose research work done during World War II remained unknown for a long time, calculated the true surface area in elastic contact of two rough bodies. He modeled spherical segments of equal radius for the microasperities whose tips were assumed to be linearly distributed and obtained

$$A = K \left( \frac{1-\nu^2}{\pi E} \right)^{10/11} N^{10/11} \quad (1)$$

where  $K$  is a coefficient,  $E$  is modulus of elasticity, and  $\nu$  is Poisson's ratio. Greenwood and Williamson (Ref. 7) derived the following relationship assuming elastic contacts.

$$A = \pi \gamma A_a r \sigma F_I(h) \quad (2)$$

where

- $\gamma$  = density of asperities
- $A_a$  = nominal contact area
- $r$  = radius of asperities
- $\sigma$  = standard deviation of height distribution of asperities
- $h$  =  $d/\sigma$

$$F_I(h) = \int_h^{\infty} (s-h)^n \phi^*(s) ds \quad (3)$$

where  $\phi^*$  represents the normal density distribution of heights of asperities, (i.e.  $\phi^*$  is the height distribution scaled to make its standard deviation unity), and  $d$  represents the distance between the reference planes in each contacting surface (see Fig. 2). It is assumed that all asperity summits have the same radius  $r$  and their heights vary randomly. Figure 3 shows the manner in which the contact area may vary when the interfaces are under "very high pressure". It may be noted that the true area of contact under "moderate loads" can be less than 50% of the possible total area.

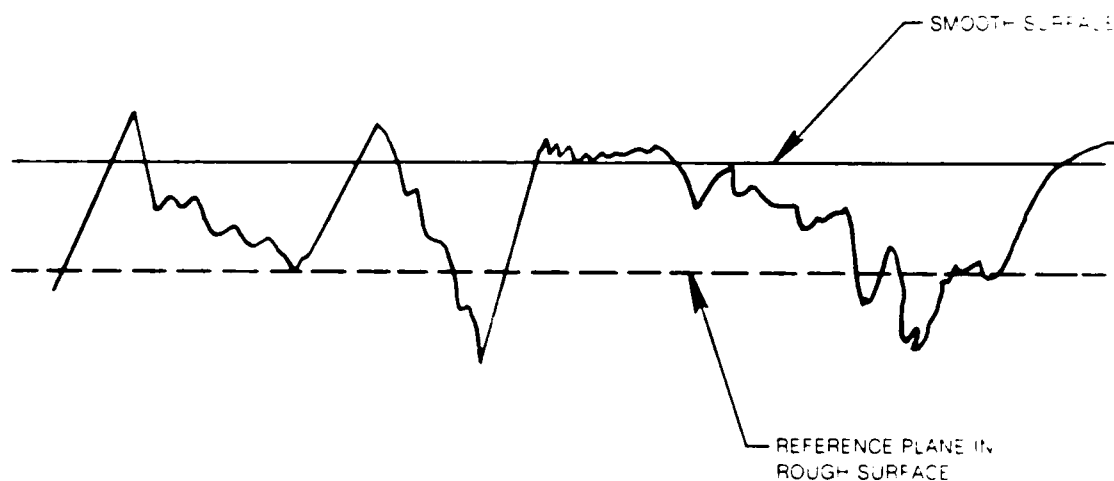
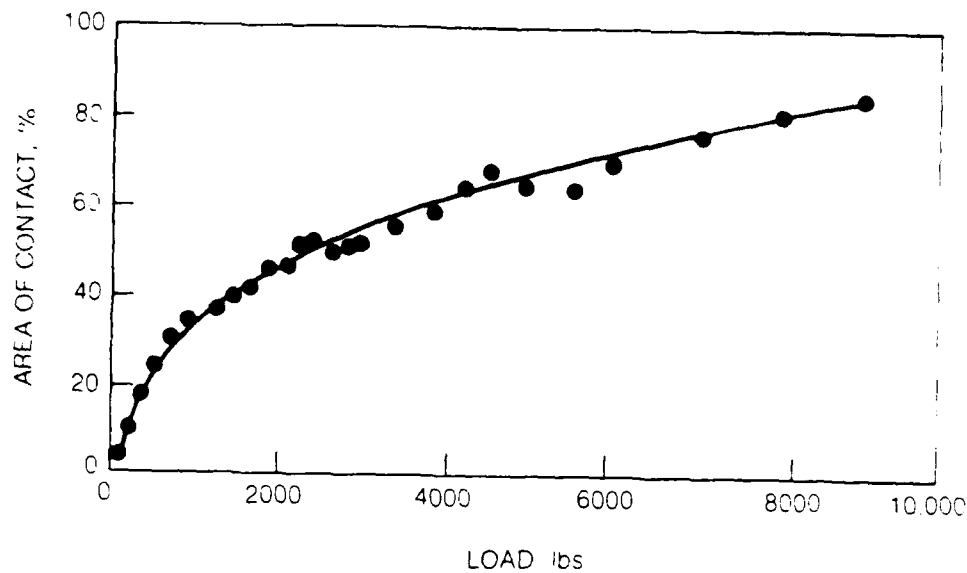


Figure 2. Surface Characterization



REF #4 PAGE 109

**Figure 3. Behavior of Contact Under Very High Pressure**

Oden and Pires, in Ref. 8 also present a simple argument to demonstrate that the contact area should vary, approximately, linearly with the normal load. In general, the contact pressure will be a constant independent of the deformation. The total contact area,  $A_c$ , can be represented as

$$A_c = A_1 + A_2 + \dots + A_n \quad (4)$$

where  $A_K$  is the contact area at point K and n is the total number of contact points. Then the normal force at point K is given by

$$N_K = p_o A_K \quad (5)$$

where  $p_o$  is the yield pressure for the material. Substituting for the areas in Eq. (4),

$$A_c = \frac{N_1}{p_o} + \frac{N_2}{p_o} + \dots + \frac{N_n}{p_o} = \frac{N}{p_o} \quad (6)$$

where N is the total normal force.

Figure 4 shows the nature of deformation of the asperities as the normal load increases. The symbols in Fig. 4 refer to the height of the asperities in microinches below which a certain percentage of the surface lies. As the load increases, the highest points at the interface flatten as expected. But the upward slopes in the data show that heights of asperities actually increase indicating an elastic deformation of the entire surface. Clearly, any law of friction at interfaces must account for the deformation taking place in the neighborhood of a point in question.

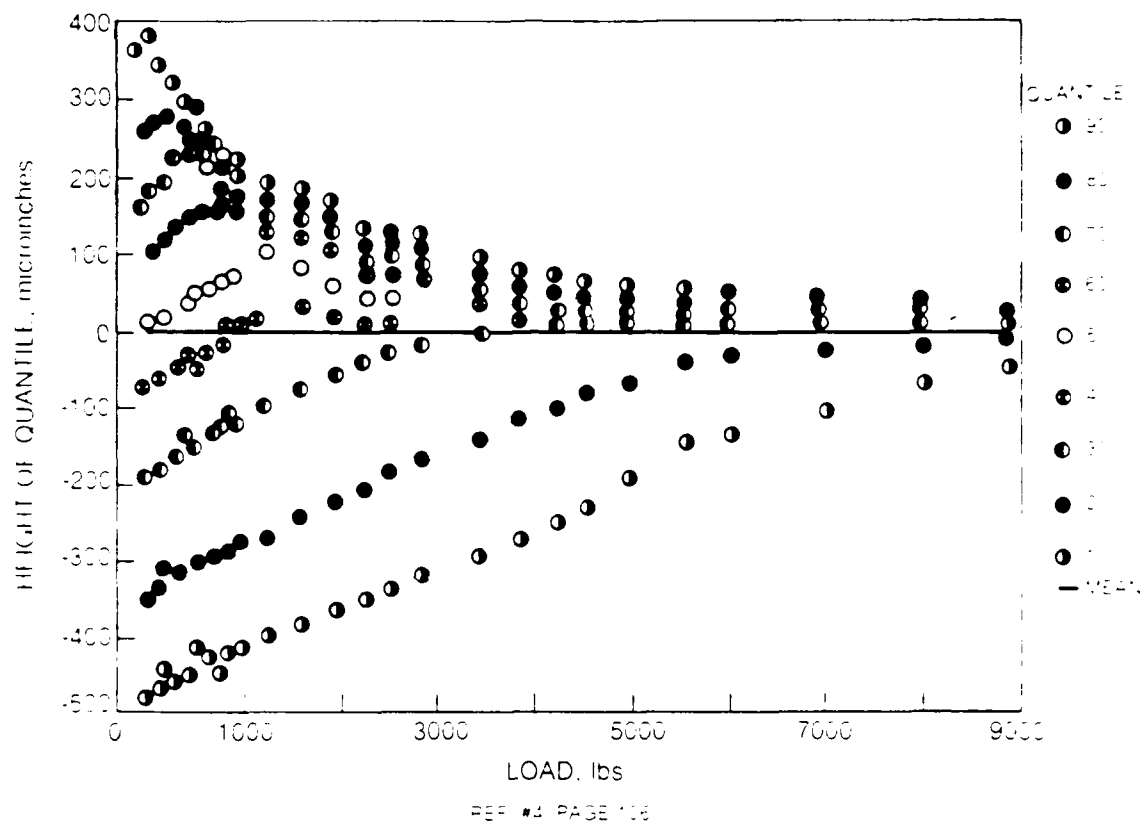
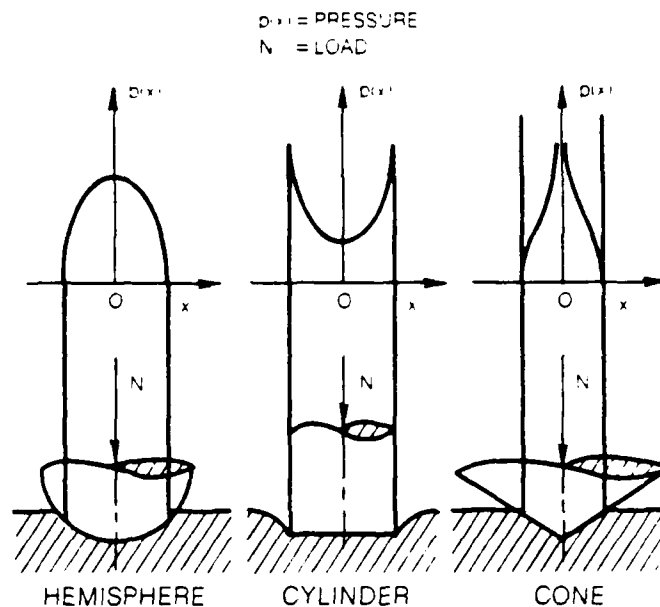


Figure 4. Behavior of Aluminum Surface Under High Pressure Contact

Most of the researchers who have tried to characterize the asperities appear to agree on the spherical segment as the most convenient geometry to model surface roughness. The preference for this simple geometry is obvious in view of indeterminate stress distribution calculated for other geometries examined, i.e. a bar model and a cone model as shown in Fig. 5.



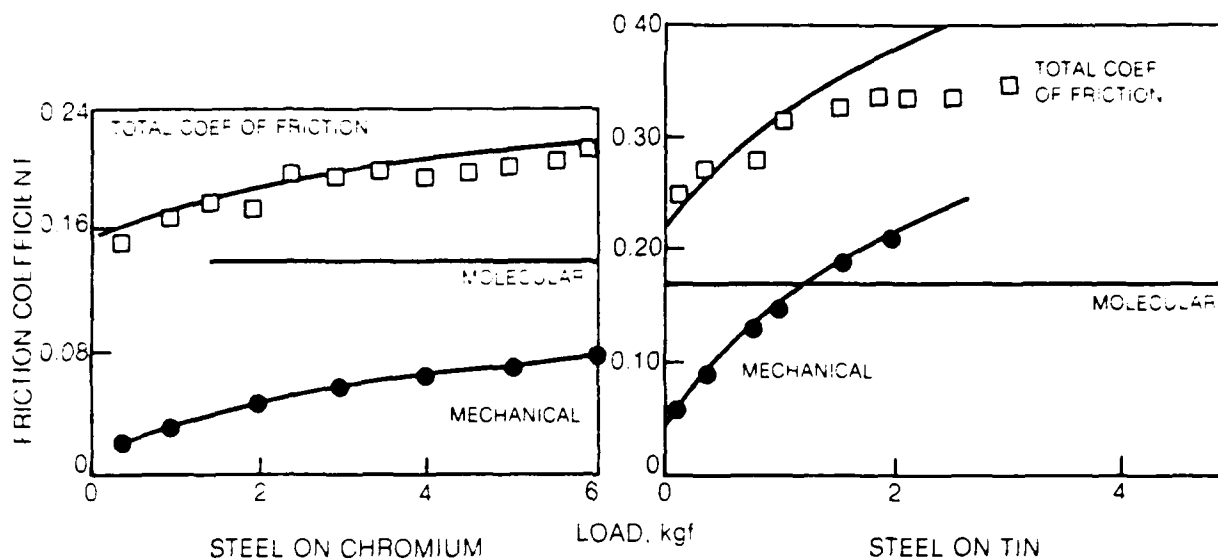
REF #1 PAGE 57

**Figure 5. Comparison of Pressure Distribution Curves Obtained in the Contacts of Various Geometric Shapes**

If an ellipsoidal geometry is considered appropriate, a radius for an equivalent sphere is calculated from  $r_{eq} = \sqrt{r_{long} r_{tran}}$ .

## 2.2 Characteristics of Friction Forces

A great variety of phenomena occur in rubbing contact between surfaces of components. This is because of the dual nature of friction by which surface friction overcomes molecular interaction forces between surfaces and mechanical resistances associated with changes in the profile of the surface layer. Kragelsky et al (Ref. 1) point to data that indicates molecular attraction at an interface could contribute substantially to the observed frictional forces. As can be observed from Fig. 6, the contribution to friction from molecular forces can dominate particularly for lighter load conditions. It is assumed that a sublayer of decreased resistance is formed at the interface between rubbing components. One speaks of dry friction forces when the sublayer is in a solid phase.



REF \*\* PAGE 192

**Figure 6. Variation of Friction Coefficient Components with Normal Load**

Mechanical deformation may occur due to either penetration of surfaces with ploughing or continuous formation and rupture of welds. As stated earlier, all these processes are influenced by the environment. As observed by Kragelsky, et al (Ref. 1) "in spite of the complex nature of mechanical, physical, and chemical processes involved, it is still possible to pinpoint certain principles which are common to all friction and wear processes". They are outlined below:

1. Three interconnected processes occur simultaneously in sliding contact
  - a) Interaction of the surfaces
  - b) Changes in the surface layers and films
  - c) Rupture of the surface layer.
2. The contact between solids occurs at discrete points because of surface roughness.
3. Increase in load leads to increase in contact area due to increase in number of contact points. Therefore, the real pressure at any point increases only slightly.



4. Tangential resistances are additive. Dissipation of energy in the formation and rupture of an individual frictional bond is determined by the resistance in overcoming molecular interaction at points of contact, and the mechanical ploughing effects.

5. Surface sliding requires formation and rupture of a thin layer (weakened layer of base material or films) whose shear strength must be less than the shear strength of the substrate.

The apparent simplicity of the relationship that friction force induced at a point on an interface is proportional to the normal load at that point has been the primary reason for its use in most studies of dry friction. However, in addition to the problem of obtaining a reliable estimate of the constant of proportionality, i.e. the coefficient of friction  $\mu$ , the representation  $F = \mu N$  leads to computational complications even when applied to the study of a single degree-of-freedom system (see Fig. 7), as shown by Den

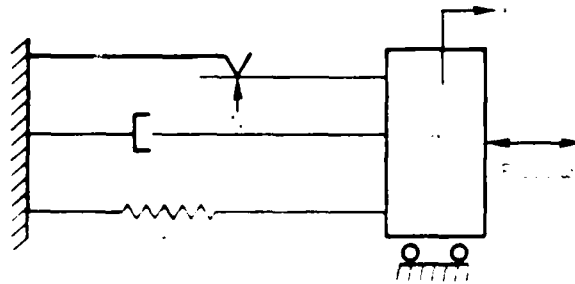


Figure 7. Den Hartog's Model

Hartog (Ref. 9). Oden and Pires (Ref. 8) have recently discussed the mathematical and physical difficulties associated with such a representation. Nevertheless, a substantial number of attempts have been made and continue to be made to use modifications of this basic model as shown in Fig. 8 (Refs. 10 to 26). Such modifications are adaptations of the basic model to the analysis of particular components under study. Adding more degrees-of-freedom to the basic model leads to additional complexity (Ref. 10) which can be avoided by the use of linearized versions of the model. As shown by Jacobsen (Ref. 11), such linearization can provide a good representation of system behavior if the friction force is small so that it does not distort the motion appreciably. Subsequent analyses, many of which have been devised to represent specific

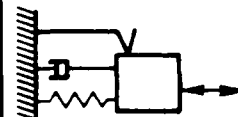
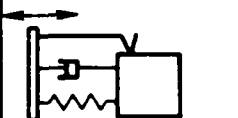
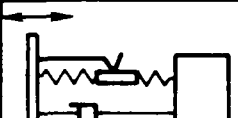
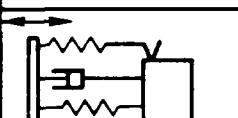

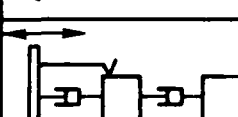

| STRUCTURAL/<br>MECHANICAL<br>MODEL | FRICTION<br>MODEL &<br>FORM OF<br>SOLUTION |  |  |  |  |  |  |  | OTHER<br>LUMPED<br>MASS     | CONTINUUM<br>eg BUILT-UP<br>BEAM   | NON-RESONANT<br>eg SIMPLE<br>LAP JOINT                     |
|------------------------------------|--|---|---|---|---|---|---|---|-----------------------------|--|--|
|                                    |  | JACOBSEN<br>(11)  | LEVITAN<br>(24)   | SRINIVASAN<br>(14)  | GRIFFIN (13)<br>SRINIVASAN (14)   | PRATT/WILLIAMS<br>(12)  | YEH<br>(10)   | ANTONIOU<br>ET AL (22)<br>$\mu = \mu(q)$  | EARLES/<br>WILLIAMS<br>(16) | BEARDS (23)<br>REVIEW  | GOODMAN<br>(26)<br>GOODMAN (18)<br>REVIEW<br>ANNIGERI (20) |
| I LINEARIZED                       |  |   |   |   |   |   |   |   |                             |  |  |
|                                    | a) STEADY STATE                            |   |   |   |   |   |   |   |                             |  |  |
|                                    | b) TRANSIENT                               |   |   |   |   |   |   |   |                             |  |  |
| II. COULOMB                        |  | DEN HARTOG<br>(9)   |   |   |   |   |   |   | MAYES/<br>MOWBRAY<br>(15)   |  |  |
|                                    | a) STEADY STATE                            |   |   |   |   |   |   |   |                             |  |  |
|                                    | b) TRANSIENT                               |   |   |   |   |   |   |   |                             |  |  |
| III VARIABLE $\mu$                 |  |   |   |   |   |   |   |   |                             |  |  |
|                                    | a) STEADY STATE                            |   |   |   |   |   |   |   |                             |  |  |
|                                    | b) TRANSIENT                               |   |   |   |   |   |   |   |                             |  |  |
| IV CONSTANT $\mu$                  |  |   |   |   |   |   |   |   |                             | BEARDS (23)<br>(REVIEW)<br>PIAN (17)<br>RIMKUNAS/FRYE(21)<br>BIELAWA(19) | GOODMAN<br>(26)<br>GOODMAN (18)<br>REVIEW<br>ANNIGERI (20) |
|                                    | 1st CYCLE ONLY                             |   |   |   |   |   |   |   |                             |  |  |
| V. VARIABLE $\mu$                  |  |   |   |   |   |   |   |   |                             |  |  |
|                                    | 1st CYCLE ONLY                             |   |   |   |   |   |   |   |                             |  |  |
| VI CONSTANT $\mu$                  |  |   |   |   |   |   |   |   |                             |  | GOODMAN (18)<br>(REVIEW)                                   |
|                                    | 1st CYCLE TO<br>STEADY STATE               |   |   |   |   |   |   |   |                             |  |  |
| VII VARIABLE $\mu$                 |  |   |   |   |   |   |   |   |                             |  | EARLES/PIHOT<br>(25)                                       |
|                                    | 1st CYCLE TO<br>STEADY STATE               |   |   |   |   |   |   |   |                             |  |  |
| UNIFORM GROSS SLIP                 |  |   |   |   |   |   |   |   |                             |  |  |
| MICROSLIP                          |  |   |   |   |   |   |   |   |                             |  |  |

Figure 8. Dry Friction Damping Models

vibratory components, have generally relied upon the basic model in its linearized version. These developments have mainly involved more degrees-of-freedom and different configurations (Refs. 12, 13, 14, 15). Improved friction models have been tried, for example, making the friction force dependent on the vibration amplitude (Ref. 16) and by analyzing the interfacial slip in a vibrating beam (Ref. 17). However, there have been few studies which incorporate a detailed model of interface behavior into a model of a vibrating system.

In 1778, a two term formula was proposed by Coulomb according to which the friction force  $F$  was written as  $F = AN+B$ , where  $A$  can be identified as the familiar coefficient of friction. With such a representation, the coefficient of friction is not a property depending only on the materials in contact but also on the normal load.

Interface behavior is a difficult area of study which is why it is often avoided by invoking a constant overall coefficient of friction. Any discussion of friction in the context of vibratory rub must recognize the need to distinguish between the tangential forces of external static friction and those of external dynamic friction. The former exist in a region of small partially reversible displacements and peak at the boundary of such a region. Dynamic friction forces are not dependent on the magnitude of displacement. The fully developed static friction force is characterized by a coefficient which is different from that corresponding to the dynamic friction force. In the solution of vibration problems, prior to the initiation of any sliding motion, the static coefficient of friction should govern. The coefficient of friction is either chosen on the basis of practical experience or used as a disposable parameter to obtain the best agreement between theory and experiment. However, a deeper understanding of the effects of interface damping on vibrating systems can only be obtained by studying the friction processes in more detail.

Introducing the concepts of a local coefficient of friction and combining it with a study of stress distribution in the contact leads to a microslip solution in which only a part of the contact undergoes relative motion. Goodman (Ref. 18) has reviewed the basis of this approach which has since been applied to practical systems through the use of finite element techniques (Refs. 19, 20, 21).

Postulating an overall friction force, but allowing it to vary throughout each vibration cycle leads to the study of stick-slip behavior. Antoniou et al (Ref. 22) have reviewed this approach and show the degree of complication which this can add to a one degree of freedom system.

The classical mathematical model of dry friction, i.e.

$$F = \begin{cases} + F_0 & ; \dot{x} > 0 \\ - F_0 & ; \dot{x} < 0 \end{cases} \quad (6)$$

(where  $F_0$  is the force of slipping friction,  $\dot{x}$  is the velocity of slipping) leads to a force-displacement relationship for alternating input displacement illustrated by two fixed horizontal lines and two vertical lines as shown in Fig. 9. Experimental observations, however, suggest that the transition from

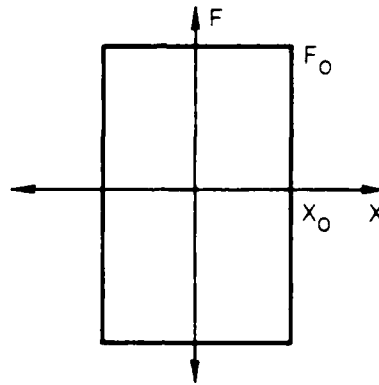


Figure 9.

one equation of slip ( $-F_0$ ) to the other ( $+F_0$ ) is smoother than indicated by Eq. (6), and more like the characteristics shown in Fig. 10 (see Ref. 27).

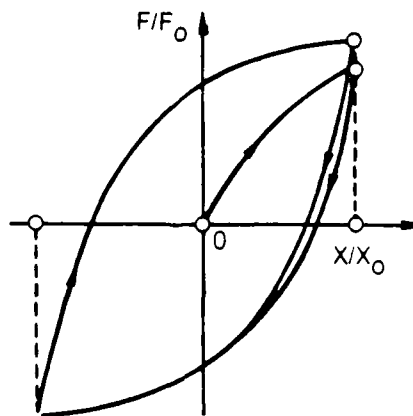


Figure 10. Hysteresis Characteristic of Dry Friction

This important observation allows the introduction of hysteresis characteristics of contact interaction and may serve as a basis of the analysis of friction damping. Accordingly, if  $x$  and  $F$  represent displacement and friction force respectively and  $x_0$ ,  $F_0$  their maximum values, the hysteresis representation may be represented as

$$\alpha = \begin{cases} 1 - e^{-\beta(\xi - C_1)} & ; \dot{\xi} > 0 \\ -1 + e^{\beta(\xi - C_2)} & ; \dot{\xi} < 0 \end{cases} \quad (7)$$

where

$$\begin{aligned} \alpha &= F/F_0 \\ \xi &= x/x_0 \\ \beta &= bx_0 \\ b &= \text{is a material constant} \end{aligned}$$

The constants  $C_1$ ,  $C_2$  can be shown to be equal and opposite to each other, i.e.,  $C_1 = -C_2$

$$\therefore \frac{d\alpha}{d\xi} = \begin{cases} \beta(1-\alpha) & ; \dot{\xi} > 0 \\ \beta(1+\alpha) & ; \dot{\xi} < 0 \end{cases} \quad (8)$$

Given initial values of  $\xi$ ,  $\alpha$ , the constants  $C_1$ ,  $C_2$  can be generated for the ascending and descending parts of the loop. The procedure can be repeated for several vibration cycles.

An amplitude dependent model of friction can be derived as shown in Ref. 23 for any prescribed value of  $\beta$ . For example, for  $\xi = A$ , from Eq. (7)

$$\alpha_A = 1 - e^{-\beta(A - C_0)} \quad (9)$$

$$\alpha_{-A} = -1 + e^{\beta(-A + C_0)}$$

which leads to 
$$C_0 = \frac{-1}{\beta} \ln (\cosh \beta A) \quad (10)$$

using which  $\alpha$  can be shown to be

$$\alpha = \begin{cases} 1 - \frac{e^{-\beta\xi}}{\cosh \beta A} & \dot{\xi} > 0 \\ -1 + \frac{e^{\beta\xi}}{\cosh \beta A} & \dot{\xi} < 0 \end{cases} \quad (11)$$

Equation (11) is an amplitude dependent friction model. The area of the hysteresis loop due to friction can be shown to be equal

$$4(A - \frac{1}{\beta} \tanh \beta A) \quad (12)$$

from which  $\beta$  can be determined from tests. It may be noted that  $4A$  in the above expression is the area of the loop consistent with the friction characterization shown in Eq. (6).

An appreciation of the continuum nature of bodies in contact leads to the concept of nonlocal laws of friction postulated by Oden and Pires (Ref. 8). With such a representation, the friction force at a point  $\bar{x}$  is the sum total of the influence of normal stresses over a neighborhood as shown schematically in Fig. 11. Thus, unlike the local law

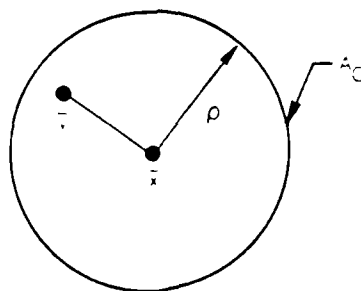


Figure 11. Nonlocal Nonlinear Laws of Friction (Oden & Pires)

$$\tau(\bar{x}) = \mu \sigma_n(\bar{x}) \quad (13)$$

a nonlocal law represents

$$\tau(\bar{x}) = \mu \int_{A_c} w_\rho(\bar{x}-\bar{y}) \sigma_n(\bar{y}) dA_c \quad (14)$$

where  $W_\rho$  is a weighting function that distributes the influence of  $\sigma_n$  in a circle of radius  $\rho$ . Recognition of the fact that the friction (shear stress) vector is always opposed to the direction of relative motion leads to the modification of Eq. (14) as follows,

$$\bar{\tau}(\bar{x}) = -\mu \bar{n}_f \int_{A_c} W_\rho(\bar{x}-\bar{y}) \sigma_n(\bar{y}) dA_c \quad (15)$$

$$\bar{n}_f = \frac{\bar{u}_f}{|\bar{u}_f|}$$

where  $\bar{u}_f$  is the vector of relative displacement along the surface. A more complete representation is achieved by introducing the requirement that the friction force be dependent on the motion (displacement or velocity) and leads to

$$\bar{\tau}(\bar{x}) = -\mu \bar{n}_f \phi_e(u_f) \int_{A_c} W_\rho(\bar{x}-\bar{y}) \sigma_n(\bar{y}) dA_c \quad (16)$$

Figures 12 and 13 show possible representation of  $W$  and  $\phi$ .

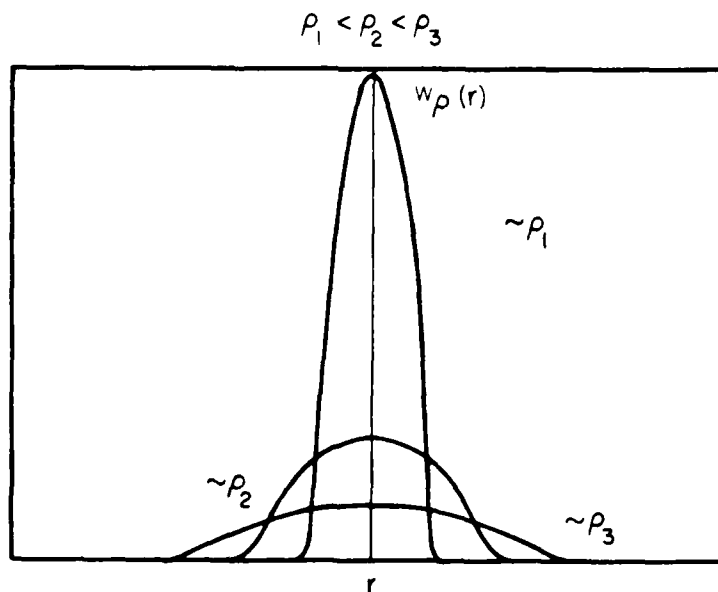


Figure 12. Nonlocal Effects

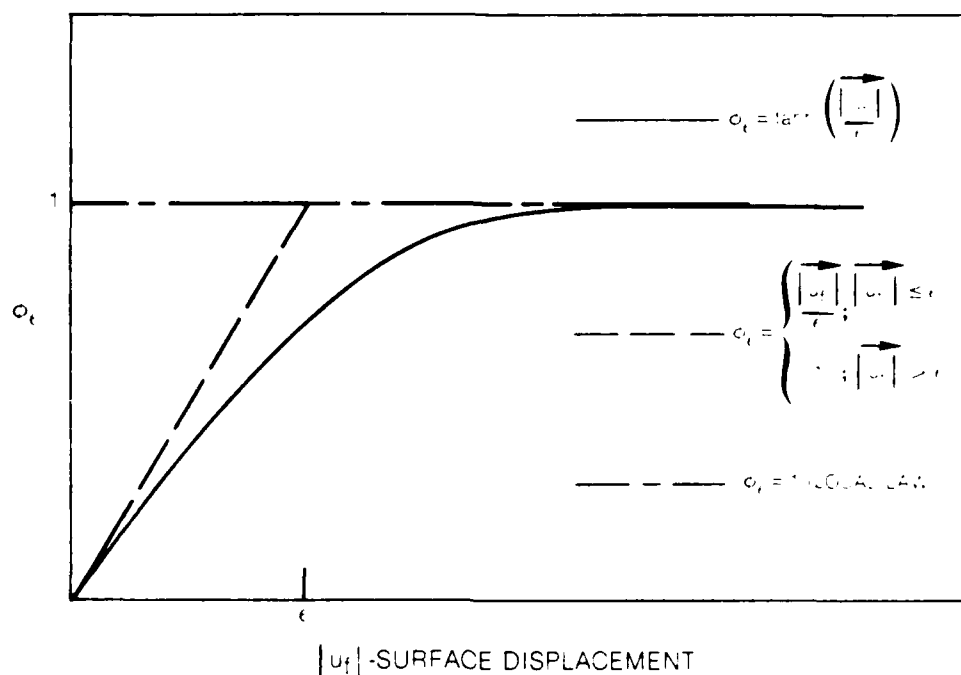


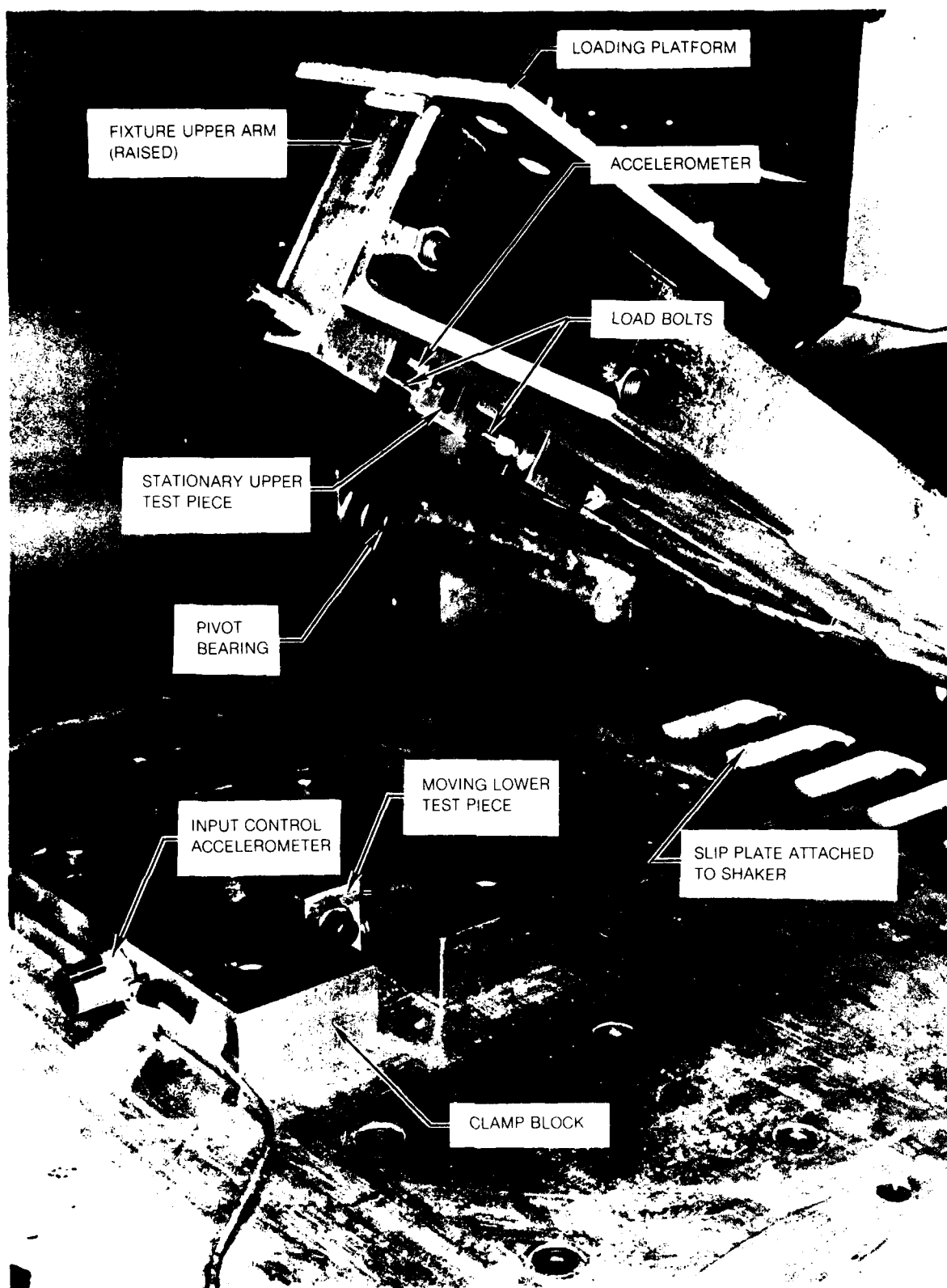
Figure 13. Nonlinear Effects

#### 2.2.1 Coefficient of Friction

An accurate calculation of friction forces induced at interfaces in relative vibratory motion depends on the accuracy with which the coefficient of sliding friction can be estimated. As observed earlier, there appears to be no experimental data obtained in a vibratory environment from which the nature of the coefficient of friction can be obtained. The following is a summary of such an experiment performed at the United Technologies Research Center under contract to NASA LeRC (Ref. 14).

The approach that was chosen in that investigation was to provide sinusoidal relative motion between two test pieces which were held together with a constant normal force and to measure the resulting frictional forces directly. The range of normal loads, frequencies and relative velocities imposed were consistent with vibration of a jet engine fan in which resonant vibration is partly limited by damping available due to rubbing at shroud interfaces. The test pieces were a pair of titanium alloy (8-1-1) bars with their rubbing interfaces flame sprayed with tungsten carbide. The size of the rubbing surface was 22.35 x 6.35mm. The test assembly, shown in Figs. 14 and 15 uses an electrodynamic shaker to induce sinusoidal excitation of the lower test piece. The upper piece which rubs on the lower piece during test was held in such a way that longitudinal forces on the piece could be measured using a strain gaged load bolt, without any appreciable movement. The normal load on the joint was applied by setting the required weights on the loading platform. Testing consisted of setting the required frequency and input





**Figure 14. Friction Test Assembly (Upper Arm Raised)**



Figure 15. Friction Test Assembly

acceleration and recording the frictional force-slip loop on an oscilloscope for a range of normal loads.

The nominal condition for testing was defined as a displacement of 0.127mm DA at a frequency of 280Hz with normal loads ranging from about 250 to 700N. Three loads were used, based on the weights available and the dead load of the upper arm; these were 271, 492, and 672N. The displacement was varied from 0.056 to 0.132mm DA and frequencies of 80, 140, 280 and 420Hz were input. Two typical friction force-slip loops are shown in Fig. 16.

The equivalent friction coefficient was determined from the measured area of the recorded (photograph of oscilloscope picture) loop and a knowledge of the input frequency and displacement. The resulting values for friction coefficient are shown plotted against normal load, frequency and velocity, in Fig. 17. A least squares fit of an equation of the form:  $\text{coef} = (A/\text{Load}) + b$  was attempted using all the data. The resulting curve is shown superimposed on the test data points in Fig. 17. An examination of the data in Fig. 17 indicates that there is no obvious correlation with either input frequency or maximum velocity.

### 2.3 Dry Friction Damping Technology

Control of resonant vibration in light, flexible structures has been found to be largely the result of damping available at mating surfaces. The potentials of such damping depends, as has been observed earlier, on a host of parameters that include the magnitude of normal force holding the surfaces in close contact and the characteristics of the surfaces. These and other parameters determine the nature and extent of slip at the interfaces so that an optimum in energy dissipation can be expected with an appropriate combination of normal load and relative motion (Ref. 23). Therefore, an understanding of the processes involved in relative vibratory motion at joints becomes a basic requirement that may influence the design of structures where friction becomes an important source of damping.

The analytical approaches for estimating friction damping can be broadly classified as follows: (1) macroslip approach and (2) microslip approach. In the macroslip approach, the entire interface is assumed to be either slipping or stuck. The friction mechanism is either replaced by an equivalent linear viscous model or assumed to be governed by some form of Coulomb's law of dry friction. The effect of friction damping is obtained by determining the forced response of the component. The analysis involved is relatively straightforward and the justification for wide-spread use of this approach is its effectiveness at predicting the actual response. However, there is some question as to the validity of the macroslip approach when the interface has a large area, and is subject to a nonuniform load distribution. In the microslip approach, a relatively detailed analysis of the stress distribution at the interface is carried out, typically via a finite-element procedure. The extent of local slip, not necessarily throughout the interface, between

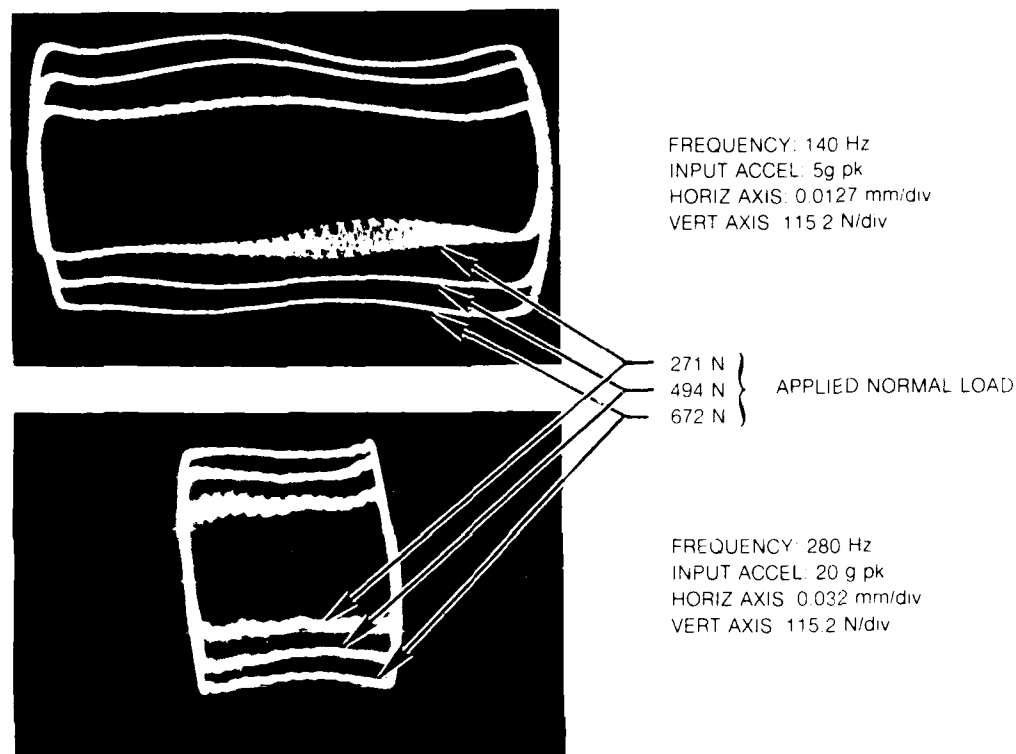


Figure 16. Typical Measured Friction Force—Slip Loops

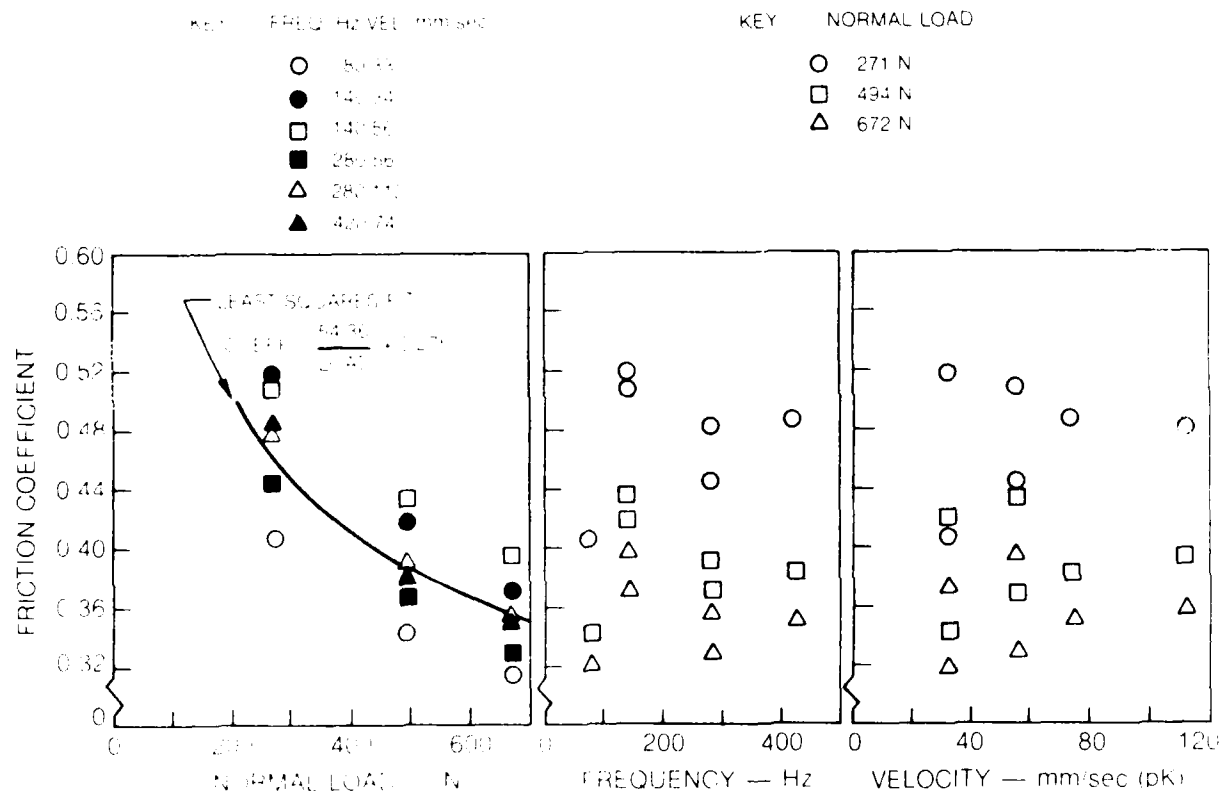
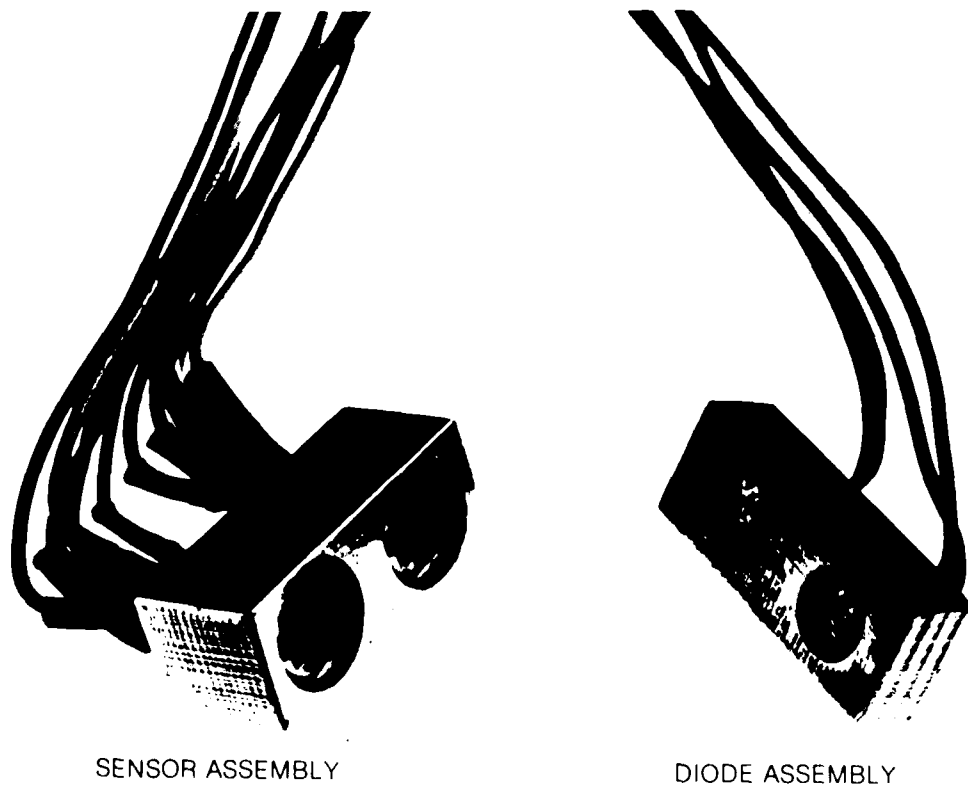


Figure 17. Variation of Equivalent Friction Coefficient During Sinusoidal Motion With Normal Load, Frequency and Maximum Relative Velocity

pairs of contacting points is determined by applying Coulomb's law of friction to the normal and tangential stresses. A detailed knowledge of interface slip dynamics can be obtained from this approach. Although much useful information can be gained in a linearized analysis, a fully nonlinear time history solution may be necessary and feasible with modern computational methods and equipment.

Calculation of energy dissipation over a period of vibration requires an accurate assessment of both the forces and motion of an interface. Much effort will be needed before satisfactory analytical models become available to calculate these parameters. In the meantime, the process of developing and calibrating analytical models requires advances in instrumentation that can measure extremely small vibratory motion at interfaces. A first step towards such development has been taken at the United Technologies Research Center and is described below.

The measurement system comprises a gallium arsenide photoemitting diode (Texas Instruments Type TIL24) and silicon position sensing detector (UDT Type PIN-SC/4D) pair mounted side by side in small aluminum block housings (see Fig. 18). The position reference is provided by the infrared LED emitting a light beam, the centroid of which is sensed by the UDT two-axes position sensing photo-detector. Each axis of the detector has two outputs which are amplified to provide adequate signal level. The voltage difference between the outputs of each axis provide the X and Y position information.



**Figure 18. Shroud Motion Measurement Device**

A feasibility study of this system was conducted to determine its potential for measuring extremely small motions at a shroud interface. A single part-span-shrouded fan blade was used and bench tests were conducted over a range of normal loads and frequencies. The installation is shown in Fig. 19.

The sensor assembly was glued using epoxy adhesive onto the shroud of a part span shrouded titanium fan blade which had its root welded into a massive titanium block. The test item was enclosed in an aluminum fixture. Application of the required normal loads on the shrouds was accomplished via loading platens mounted on a steel loading disk. The loads were set by applying a moment to the disk and then locking the disk in place. The diode assembly was mounted on the load platen opposite the sensors with a gap of 12 mils between the housings. The detector was oriented such that the Y-axis was radial and the X-axis directed along the shroud interface. The whole assembly was mounted on a slip plate attached to an electrodynamic shaker. Sinusoidal motion was applied to the blade horizontally in the direction of flap of the blade tip. The output from the motion detectors was passed through a low pass 3kHz filter and then displayed on a Tektronix DM 43 dual channel oscilloscope. Permanent records were made by photographing the resulting wave forms and Lissajous figures for each detector set.

The results of the blade tests show some interesting features of shroud motion for this particular test arrangement. The tests indicate that:

- a) Stick-slip or Coulomb damping is not evident from the traces. (A sample trace is included as Fig. 20.)
- b) Radial displacement generally exceeds that along the interface.
- c) The strain response of the blade increases with increase in shroud load indicating lower damping and yet the relative motion between the shrouds also increases.

The series of tests conducted on the single fan blade demonstrated that the optical system is very suitable for measuring small vibratory motions. It has been established that motions as small as  $50 \times 10^{-6}$  inch can be measured with this system in the frequency range of d.c. to 2kHz. The results of calibration indicate the system to be adequate for the range of frequencies and displacements that are of practical interest. This instrumentation system has been successfully used in measuring the extremely small vibratory motions at ten successive interfaces of a part-span shrouded fan. It is anticipated that in any experimental research in this area, this type of optical system will be found to be invaluable.

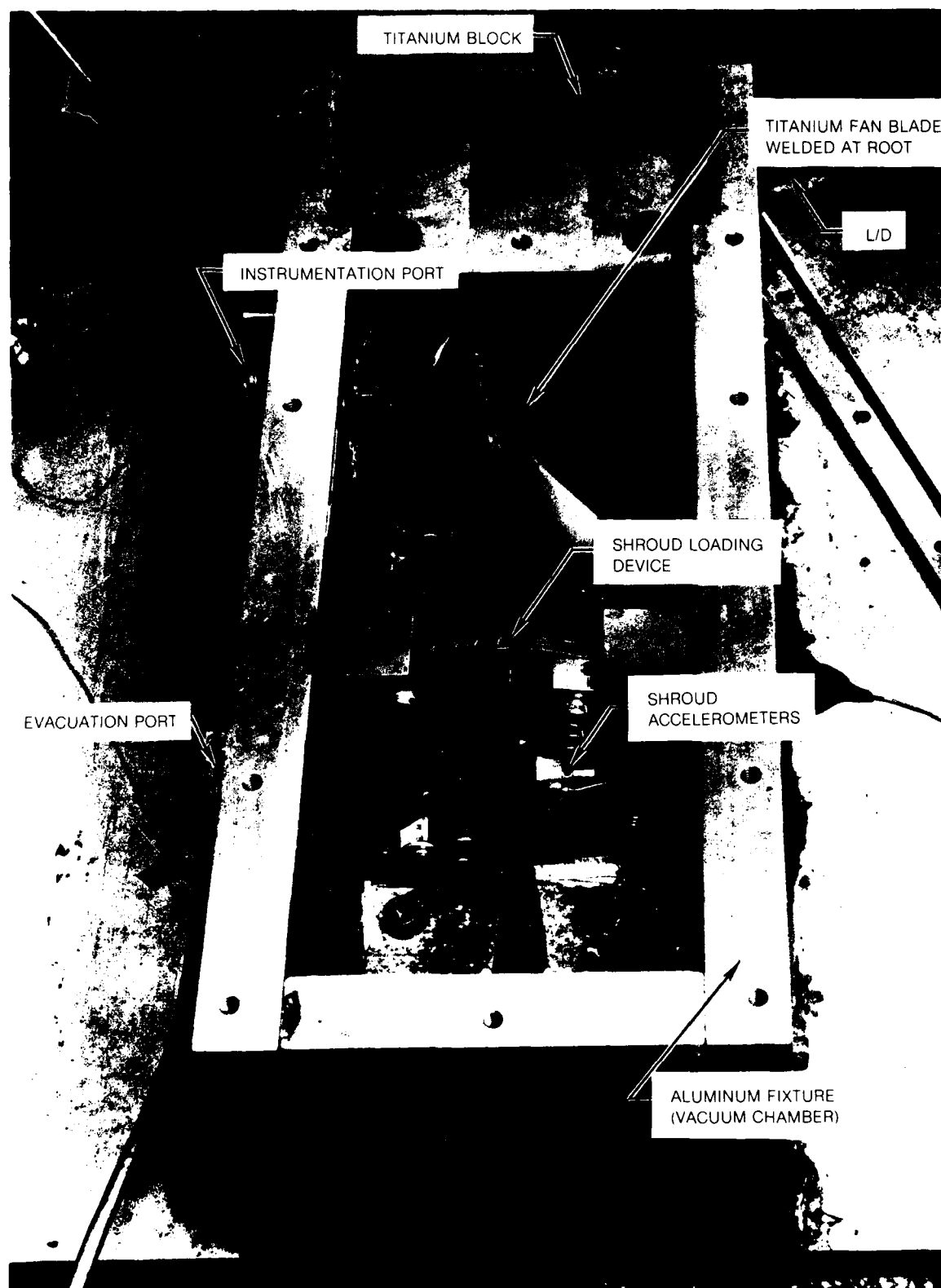
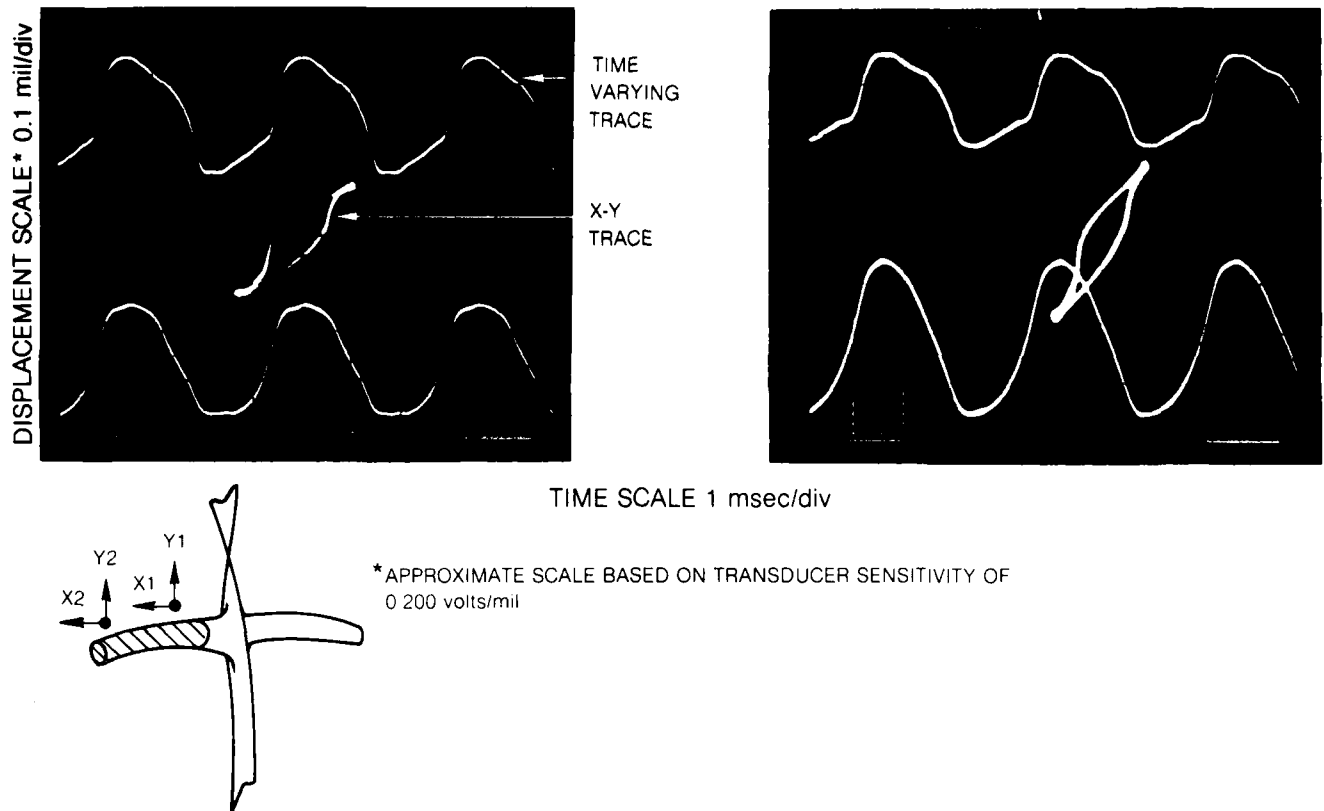


Figure 19. Test Set-Up for Shroud Damping Investigation



**Figure 20. Recorded Shroud Motions for First Mode Blade Vibration and Applied Shroud Normal Load of 34 lbs**

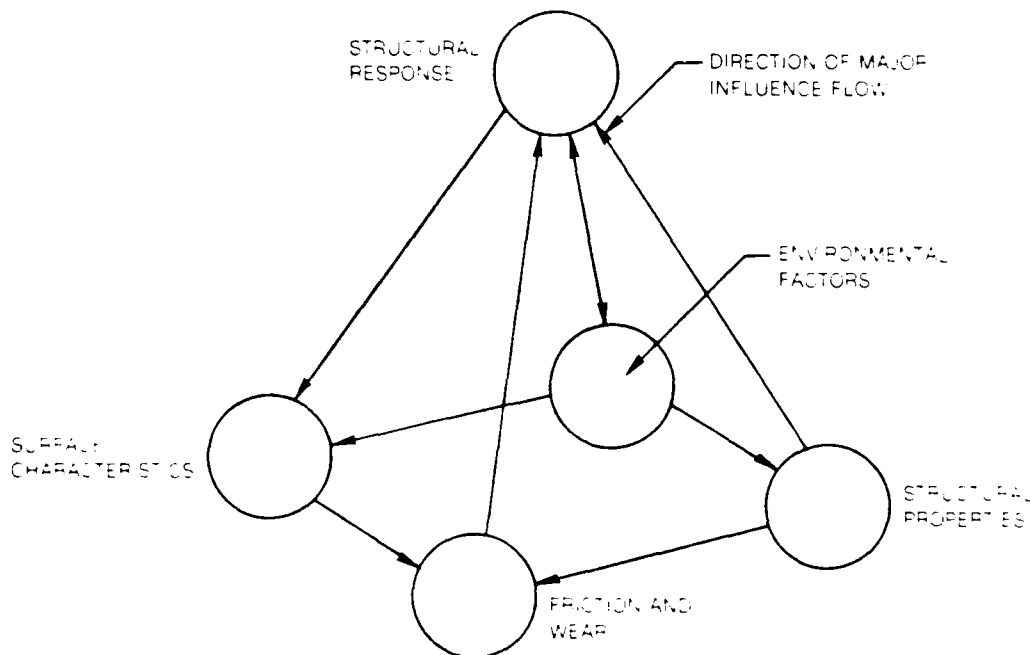


### 3. RESEARCH ISSUES AND PLANS

An accurate assessment of damping due to friction will obviously depend upon the accuracy with which the interfaces and the environment are characterized. On the basis of observations made earlier, five important interdisciplinary aspects may now be outlined.

1. Surface Science: involving a definition of the interacting surfaces in terms of (a) geometry, (b) bulk material properties such as moduli of elasticity, hardness, etc., (c) surface topography and contact area, and (d) surface chemistry.
2. Environment: involving (a) definition of mechanical and thermal loading, (b) contaminants, gases and liquids present, (c) humidity, and (d) electrical and magnetic fields.
3. Laws of friction that relate 1 and 2 above.
4. Calculation of response of a machine element using 1, 2 and 3 above along with a knowledge of structural properties such as mass, stiffness, etc.
5. Calculation of energy dissipation using 2 and 4 above.

These interdependent and influential factors may be represented in the form of a friction damping pyramid as shown in Fig. 21. Determination of



**Figure 21. Factors Influencing Structural Response When Frictional Forces are Significant**

those parameters that are most influential in a given application is an important task, although certain aspects of research in the technology of friction damping will be of a basic nature. For example, the general nature of the coefficient of friction may be established although its magnitude will vary from one pair of materials to another. Analytical modeling for both single degree of freedom and multiple degrees of freedom must be developed from first principles and calibrated on the basis of carefully planned experimental investigations. The recommended approach is shown in Fig. 22.

The single degree of freedom model that will be examined both analytically and experimentally is shown schematically in Fig. 23. Similarly, the cantilever beam of uniform cross section (see Fig. 24) with a friction joint at the root serves as a multiple degree-of-freedom system. The analytical approach that will be used in this study is described in Appendix A along with typical numerical results obtained for the SDOF model. The aim of the experimental effort in regard to both those models will be to develop a vibratory data base that can be used to (a) calibrate the analytical modeling, (b) assess the importance of various parameters and (c) quantify the extent of damping available.

As noted earlier, an important aspect of friction analysis is the determination of the law of friction that is valid and appropriate for application to a given vibrating component. The representation in the form of a nonlocal law affords the flexibility needed in this complex problem area. The representation suggested by Oden (Ref. 8) was primarily intended for the analyses of contact problems and therefore does not include provisions for gross sliding and vibratory motion. Further, in such a representation, the points on an interface of a vibratory component approach a zero relative velocity, and thus no provision is made for the velocity dependence of frictional forces. However, this concept provides a rational basis for deriving more general empirical descriptions which are appropriate to a vibratory environment.

A possible modification of Oden's nonlocal friction law is developed below and will be examined further during the course of this study. The modification shown below incorporates the nonlinear function  $\phi$  (see Eq. (16)) into the integral, i.e.,

$$\bar{\tau}(\bar{x}, t) = -\mu_s \frac{\bar{v}}{|\bar{v}|} \int_{-\infty}^{\infty} \int_{-\infty}^{\infty} \phi \left( \frac{R(\bar{x}(t), \bar{x}_1)}{\epsilon(\bar{x}_1)} \right) w \left( \frac{\eta_1}{\rho} \right) \sigma_n(\bar{x}_1, t) \frac{dx_1 dy_1}{\epsilon_o \rho} \quad (17)$$

$$R(\bar{x}(t), \bar{x}_1) = 0 \quad t < t_1 \quad \text{where } \bar{x}(t_1) = \bar{x}_1$$

$$\dot{R}(\bar{x}(t), \bar{x}_1) = |\bar{v} - \bar{v}_1| \quad t \geq t_1$$

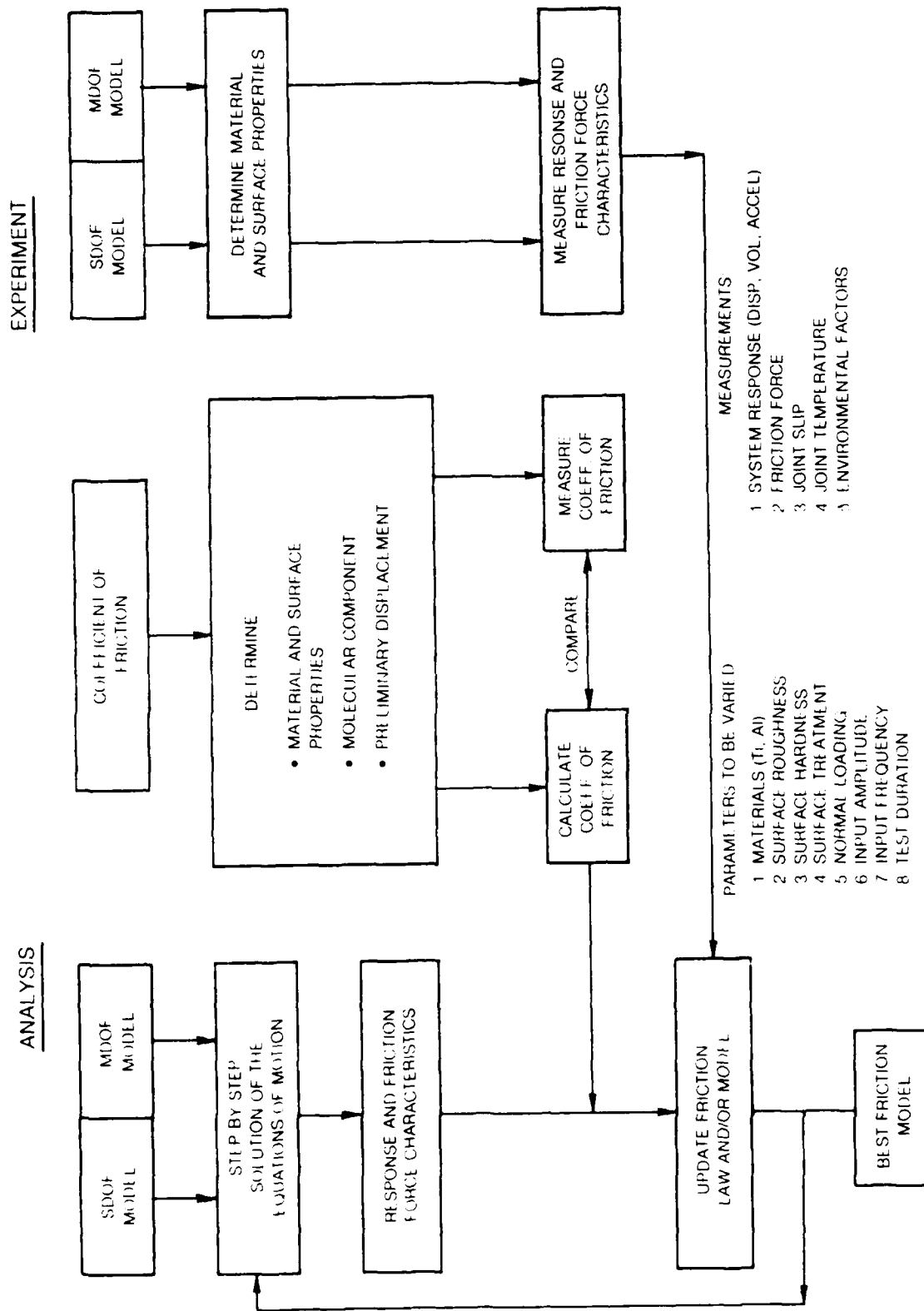


Figure 22. Dry Friction Program

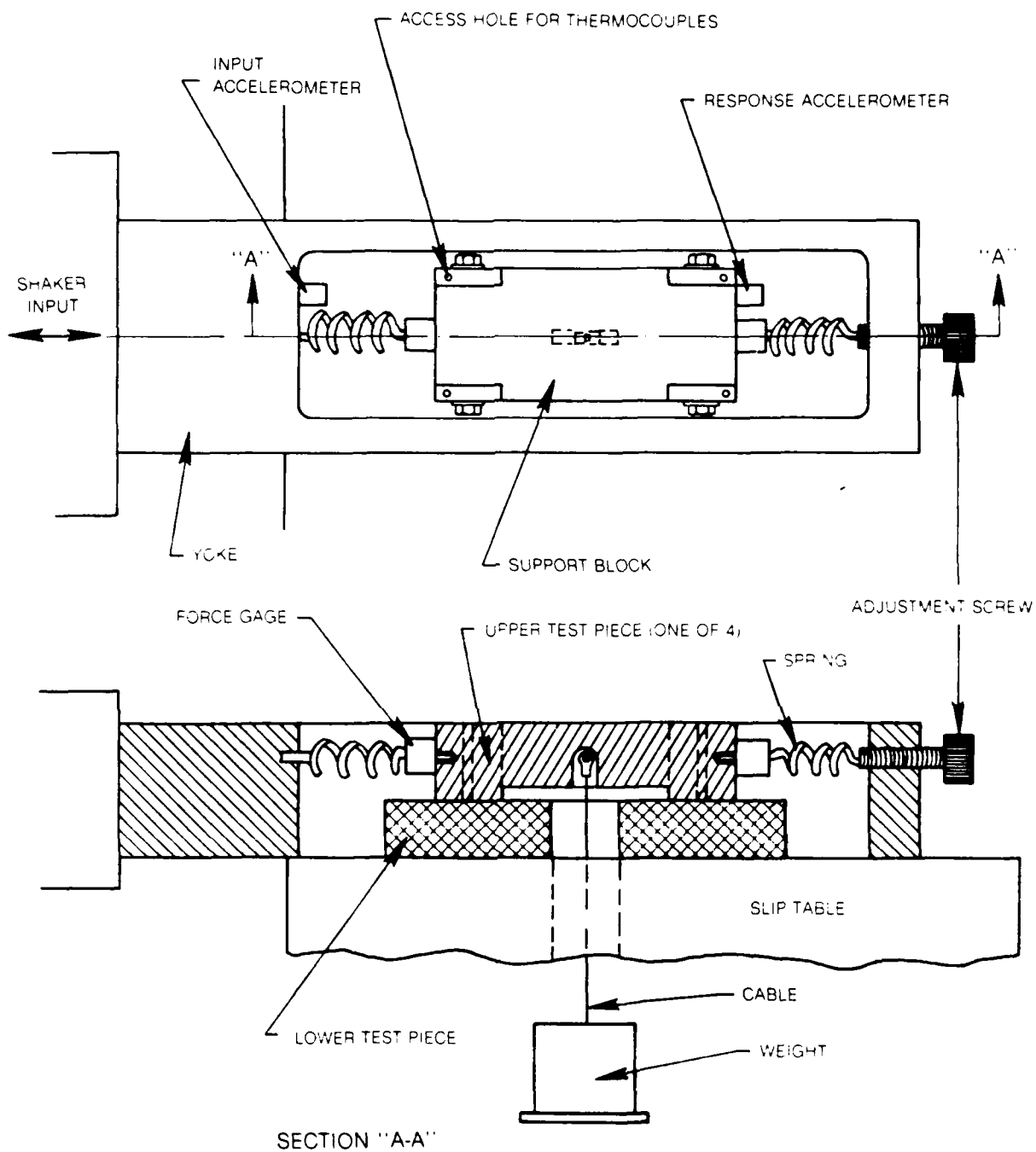
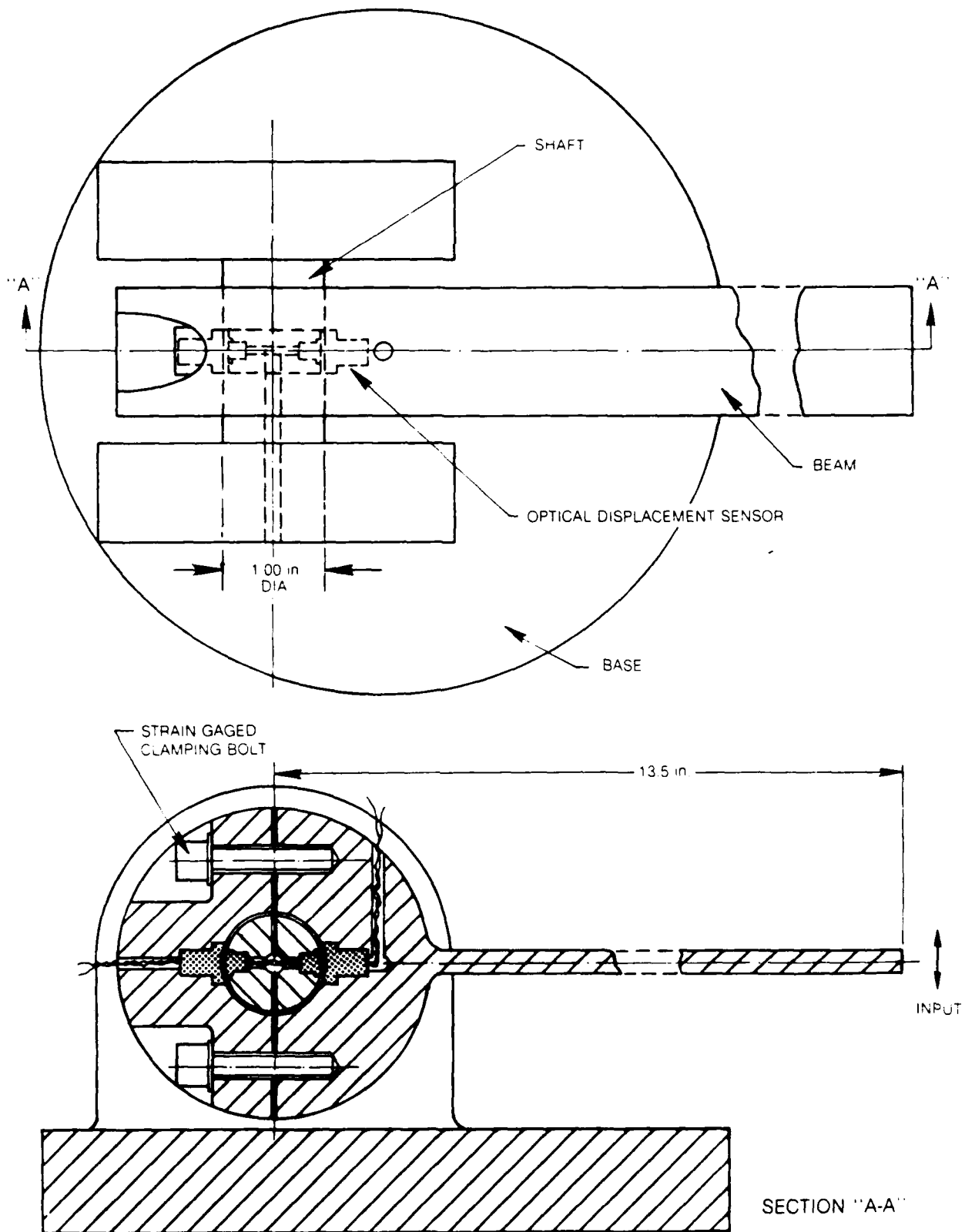


Figure 23. Schematic of SDOF Model Test Rig



**Figure 24. Schematic of MDOF Model Test Rig**

84-3-48-21

$$\dot{\epsilon}(x_1, t) = \begin{cases} 0 & t < t_1 \\ \frac{a_s}{|\bar{v}_1|} (\epsilon_0 - \epsilon) - \frac{|\bar{v}_1|}{\ell_k} (\epsilon_k - \epsilon) & t \geq t_1 \end{cases} \quad (18)$$

$$\epsilon(x_1, t_1) = \epsilon_0$$

$$\epsilon_k = \frac{\mu_k}{\mu_s} \epsilon_0$$

$$\bar{n} = \bar{x} - \frac{\bar{x} \cdot \bar{v}}{|\bar{v}|} \quad \text{is perpendicular to path of motion}$$

$$W\left(\frac{n}{\rho}\right) = \frac{e^{-n^2/2\rho^2}}{\sqrt{2\pi}} \quad (19)$$

$$\phi\left(\frac{R}{\epsilon}\right) = \frac{1}{\Gamma(p+1)} \left(\frac{R}{\epsilon}\right)^p e^{-\left(\frac{R}{\epsilon}\right)} \quad p > -1$$

$$a_s = a_0 e^{-T_a/T_{s1}}, \quad \ell_k = \ell_0 e^{T_\ell/T_{s1}}$$

where  $a_0$ ,  $T_a$ ,  $\ell_0$ ,  $T_\ell$ ,  $\rho$  are material constants and  $T_{s1}$ , is the surface temperature at  $\bar{x}_1$ .

In the characterization of surfaces between contacting bodies, it is generally assumed that the asperities are random, but generally tooling

operations place grooves on the surfaces in a preferential direction. The directional nature of these machining grooves will result in a friction force that need not align itself against the direction of relative motion. Zmitrowicz, in Ref. 28, accounts for this by representing the coefficient of friction in the form of a 2 x 2 matrix. For example, a frictional stress  $\bar{\tau}$  acting opposite to the relative surface velocities would be given by

$$\bar{\tau} = \tau_x \bar{i} + \tau_y \bar{j} \quad (20)$$

$$\begin{pmatrix} \tau_x \\ \tau_y \end{pmatrix} = - \frac{\sigma_z}{|\bar{v}|} \begin{bmatrix} \mu_{11} & \mu_{12} \\ \mu_{21} & \mu_{22} \end{bmatrix} \begin{pmatrix} v_x \\ v_y \end{pmatrix} = -\sigma_z \bar{\mu} \frac{\bar{v}}{|\bar{v}|} \quad (21)$$

where

$x, y$  are in the surface coordinates with unit vectors  $i, j$ , respectively  
 $z$  is normal to the surface  
 $v_x, v_y$  are the relative surface velocities  
 $\tau_x, \tau_y$  are the surface friction shear stresses  
 $\sigma_z$  is the normal surface stress, and

$$|\bar{v}| = \sqrt{v_x^2 + v_y^2} \quad (22)$$

when (a) the frictional shear stress is along the grooves for a relative velocity along the grooves and (b) the frictional shear stress is perpendicular to the grooves for a relative velocity perpendicular to the grooves, then the matrix  $\bar{\mu}$  can be shown to be symmetric.

## REFERENCES

1. Kragelski, I. V., M. N. Dobychin and V. S. Kombalov: Friction and Wear; Calculation Methods. Pergamon Press, Inc. 1982.
2. Kragelski, I. V., and V. V. Alisin (ed.): Friction Wear Lubrication; Tribology Handbook. Mir Publishers, 1981.
3. Panovko, Y. G., and I. I. Gubanovo: Stability and Oscillations of Elastic Systems. Consultants Bureau, New York, 1965.
4. Ku, P. M. (ed.): Interdisciplinary Approach to Friction and Wear: NASA SP-181, 1968.
5. Bowden, F. P. and D. Tabor: Friction and Lubrication of Solids: Oxford Univ. Press (London), Pt. I, 1954 and Pt. II, 1964.
6. Zhuravlev, V. A.: On the Physical Basis of the Amontons-Coulomb Law of Friction. J. Tech. Phys. (USSR), Vol. 10, 1940, p. 1447.
7. Greenwood, J. A. and J. B. P. Williamson: The Contact of Nominally Flat Surfaces. Proc. 2nd Int. Conf. on Electric Contacts (Graz, Austria), 1964.
8. Oden, J. J. and E. B. Pires: Nonlocal and Nonlinear Friction Laws and Variational Principles for Contact Problems in Elasticity. J. App. Mech., Vol. 50, 1983.
9. Den Hartog, J. P.: Forced Vibrations with Combined Coulomb and Viscous Friction. Trans. ASME, APM-53-9, pp. 107-115, 1931.
10. Yeh, G. C. K.: Forced Vibrations of a Two-Degree-of-Freedom System with Combined Coulomb and Viscous Damping. J. Acoustical Soc. of America, Vol. 39, (1966), pp. 14-24.
11. Jacobsen, L. S.: Steady Forced Vibration as Influenced by Damping. Trans. ASME, Vol. 52 (1930), pp. 169-181.
12. Pratt, T. K. and R. Williams: Non-Linear Analysis of Stick/Slip Motion. J. Sound and Vibration, Vol. 74, No. 4 (1981), pp. 531-542.



# REFERENCES (Cont'd)

13. Griffin, J. H.: Friction Damping of Resonant Stresses in Gas Turbine Engine Airfoils. ASME Paper #79-GT-109, March 1979.
14. Srinivasan, A. V., D. G. Cutts, and S. Sridhar: Turbojet Engine Blade Damping. NASA CR 165406, July 1981.
15. Mayer, R. L. and N. A. Mowbray: The Effect of Coulomb Damping on Multidegree of Freedom Elastic Structures. Earthquake Engineering and Structural Dynamics, Vol. 3 (1975), pp. 275-286.
16. Earles, S. W. E. and E. J. Williams: A Linearized Analysis for Frictionally Damped Systems. Jour. Sound and Vibration 24(4), pp. 445-458, 1972.
17. Pian, T. H. H.: Structural Damping of a Simple Built-up Beam with Riveted Joints in Bending. ASME J. Appl. Mechanics, Vol. 24 (1957), pp. 35-38.
18. Goodman, L. E.: A Review of Progress in Analysis of Interfacial Slip Damping (in Structural Damping papers from a colloquium - ASME annual meeting, December 1959), J. E. Ruzicka (ed.), Pergamon (1960).
19. Bielawa, R. L.: An Analytic Study of the Energy Dissipation of Turbo-machinery Bladed Disk Assemblies Due to Inter-Shroud Segment Rubbing. ASME Paper No. 77-DET-73 (1977).
20. Annigeri, B. S.: Finite Element Analysis of Planar Elastic Contact with Friction. ME Thesis, Graduate School of Illinois Institute of Technology (August 1976).
21. Rimkunas, D. A. and H. M. Frye: Investigation of Fan Blade Shroud Mechanical Damping. Wright-Patterson Air Force Base, Aero Propulsion Lab., Report No. FR-11065, 1979.
22. Antoniou, S. S., A. Cameron, and C. R. Gentle: The Friction Speed Relation from Stick-Slip Data. Wear, Vol. 36 (1976), pp. 235-254.
23. Beards, C. F.: The Damping of Structural Vibration by Controlled Interfacial Slip in Joints. ASME Paper 81-DET-86 (1981).

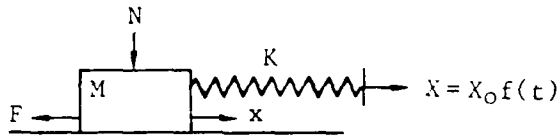
# REFERENCES (Cont'd)

24. Levitan, E. S.: Forced Oscillation of a Spring-Mass System Having Combined Coulomb and Viscous Damping. J. Acoustical Soc. of America, Vol. 32, No. 10, (October 1960), pp. 1265-1269.
25. Earles, S. W. E. and M. G. Philpot: Energy Dissipation at Plane Surfaces in Contact. J. Mech. Eng. Sci., Vol. 9 (1967), pp. 86-97.
26. Goodman, L. E. and J. H. Klumpp: Analysis of Slip Damping with Reference to Turbine-Blade Vibrations. Trans. ASME, J. Appl. Mechs., Vol. 23 (1956), pp. 421-429.
27. Busarov, Y. P. and M. S. Ostrovskii: Mathematical Model of Hysteresis of Surface Friction. Mashinovedeni 1976, No. 5, pp. 82-87.
28. Zmitrowiez, A.: A Vibration Analysis of Turbine Blade System Damped by Dry Friction Forces. Int. J. Mech. Sci., Vol. 23, No. 2, pp. 741-761, 1981.
29. Houbolt, J. C.: A Recurrence Matrix Solution for the Dynamic Response of Elastic Aircraft. J. Ae. Sc., September 1950.
30. ABAQUS Draft Manual. Hibbett & Karlsson, Inc., Providence, R.I., April 1979, revised March 1980.
31. Bathe, K. J.: ADINA: A Finite Element Program for Automatic Dynamic Incremental Nonlinear Analysis. Report 82448-1, Mechanical Engineering Department, Massachusetts Institute of Technology, Cambridge, Mass., September 1975, revised May 1977.
32. MARC General Purpose Finite Element Program, Rev. J.1. MARC Analysis Research Corporation, Palo Alto, California, 1980.
33. ANSYS Control Data Corporation, Minneapolis, Minnesota, 1977.
34. Joseph, J. A.: MSC/NASTRAN UNIVAC EDITION. The MacNeal-Schwendler Corporation, Los Angeles, California, April/May 1983.

## APPENDIX A

### SINGLE DEGREE OF FREEDOM MODEL

The objective of this study was to develop a mathematical model of a simple system incorporating nonlinear frictional elements for the purpose of (a) assisting in the design of a basic experimental rig, (b) examining the effects of different nonlinear frictional models, and (c) proving a solution method which could be applied to multi-degree-of-freedom systems. The basic model selected was a single spring-mass system with a frictional force applied directly to the block and input displacements (sinusoidal and step functions) applied to the end of the spring as shown below.



It is required to compute at any time  $t$ , the motion  $x$ , of the mass  $M$  along the axis of the spring. Acting on the mass are an input force equal to the product of the spring stiffness and the instantaneous spring extension  $(X-x)$  due to an input displacement at the end of the spring, and a frictional force  $F$ , which retards the motion.

The equation of motion for such a system when the mass is moving is shown below:

$$M \frac{d^2 x}{dt^2} = -K(X-x) - \text{sgn}(\dot{x})F \quad (A1)$$

Let  $X = X_0 f(\omega t)$

Then

$$M \frac{d^2 x}{dt^2} = -Kx + KX_0 f(\omega t) - \text{sgn}(\dot{x})F \quad (A2)$$

nondimensionalizing Eq. (A2) by letting

$$q = M \omega^2 x / KX_0, \quad \tau = \omega t, \quad s = \omega_n / \omega, \quad \omega_n = \sqrt{K/M} \quad (A3)$$

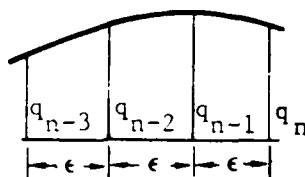
$$D = F / KX_0 \quad \text{and} \quad \ddot{q} = d^2 q / d\tau^2$$

leads to

$$\ddot{q} = f(\tau) - s^2 q - \text{sgn}(\dot{q}) D \quad (A4)$$

The method of solution applied to Eq. (A4) is one developed by Houbolt in Ref. 29. The approach is to use difference equivalents for derivatives to develop a recurrence relation that permits step-by-step calculation of the response and of the forces acting on the mass. The main feature of this recurrence approach is that the generality and physical aspects of the basic equilibrium relations of the problem are preserved without loss of ease in application. It is also applicable to nonlinear systems and MDOF systems.

By the use of difference equations, the differential equation (A4) may be transformed into an equation that involves deflection ordinates at several successive values of time. Considering a cubic curve passing through four successive ordinates time  $\epsilon$  apart, as shown below,



the following difference equations for the derivatives at the  $(n-1)^{\text{th}}$  and  $n^{\text{th}}$  steps may be obtained.

$$\dot{q}_{n-1} = (2q_n + 3q_{n-1} - 6q_{n-2} + q_{n-3})/6\epsilon \quad (A5)$$

$$\ddot{q}_{n-1} = (q_n - 2q_{n-1} + q_{n-2})/\epsilon^2 \quad (A6)$$

$$\dot{q}_n = (11q_n - 18q_{n-1} + 9q_{n-2} - 2q_{n-3})/6\epsilon \quad (A7)$$

$$\ddot{q}_n = (2q_n - 5q_{n-1} + 4q_{n-2} - q_{n-3})/\epsilon^2 \quad (A8)$$

Substituting Eq. (A8) into (A4) gives the expression for the  $n^{\text{th}}$  step value of  $q$ ,

$$q_n = (5q_{n-1} - 4q_{n-2} + q_{n-3} + \epsilon^2 f(\tau) - \epsilon^2 \text{sgn}(\dot{q}) D) / (2 + \epsilon^2 s^2) \quad (A9)$$

For the case of sinusoidal input, substituting the initial conditions  $q_0 = \dot{q}_0 = \ddot{q}_0 = 0$  at the  $(n-1)^{th}$  step into Eqs. (A5), (A6), and (A9), gives the expressions for the "first step" values of  $q$ ,  $\dot{q}$ ,  $\ddot{q}$  as

$$q_1 = (\sin \tau - \text{sgn}(\dot{q})D)/(6/\epsilon^2 + s^2)$$

$$\dot{q}_1 = 3q_1/\epsilon \quad (A10)$$

$$\ddot{q}_1 = 6q_1/\epsilon^2$$

with initial back steps

$$\begin{aligned} q_{-1} &= -q_1 \\ \text{and} \quad q_{-2} &= -8q_1 \end{aligned} \quad (A11)$$

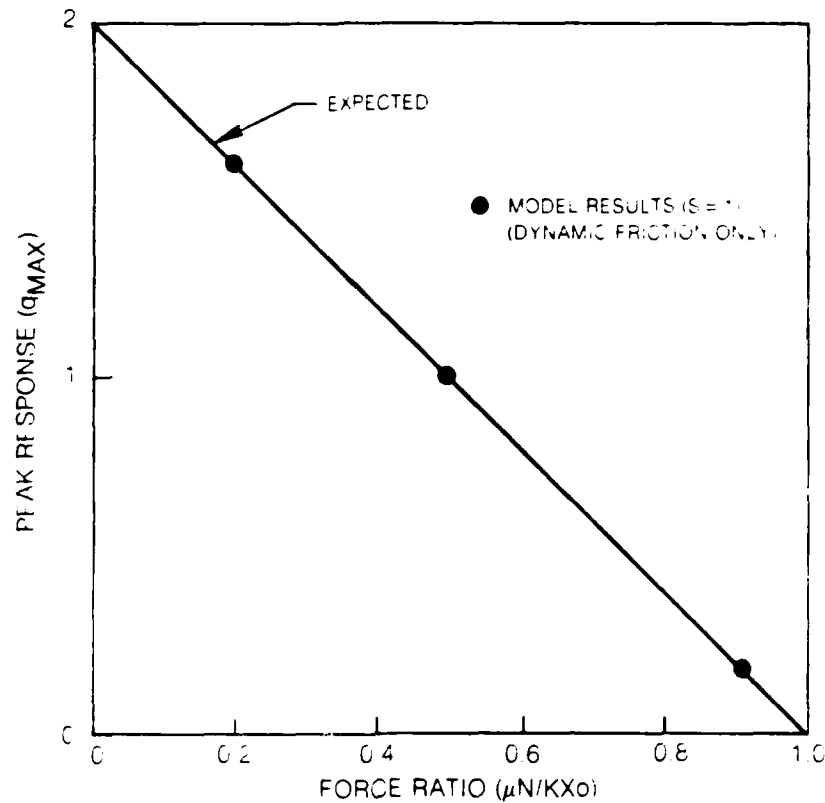
For the case of an initial spring end displacement, the initial conditions are  $q_0 = \dot{q}_0 = 0$  and  $q_0 = 1$ . The "first step" values for  $q$ ,  $\dot{q}$  and  $\ddot{q}$  are given by

$$\begin{aligned} q_1 &= (2 + f(\tau) - D)/(6/\epsilon^2 + 1) \\ \dot{q}_1 &= 3q_1/\epsilon - \epsilon/2 \\ \ddot{q}_1 &= 6q_1/\epsilon^2 - 2 \end{aligned} \quad (A12)$$

with initial "back step" values

$$\begin{aligned} q_{-1} &= \epsilon^2 - q_1 \\ \text{and} \quad q_{-2} &= 6\epsilon^2 - 8q_1 \end{aligned} \quad (A13)$$

The above expressions have been programmed in BASIC for use on an HP 9816 computer with the provision for detecting when the block comes to rest instantaneously by determining when the velocity falls below a small value. This provision is required in the case of a Coulomb type friction model where the values of static and dynamic friction coefficients are unequal. Based on preliminary studies, two sets of results have been selected for presentation. Figure A1 shows the results of an initial step displacement applied to the end of the spring. Decrease in the parameter  $D = (\mu N/KX_0)$  is equivalent to an



**Figure A1. Variation of Peak Response of SDOF Coulomb Friction Model with Initial Force Ratio for Step Input in Displacement**

increase in displacement step for constant frictional force ( $\mu N$ ). It is assumed here that static and dynamic friction coefficients are equal. Since the system is linear, the expected results can be drawn ranging from a maximum response of 2 for no friction to zero for the situation where the frictional force exceeds the initial spring force. The numerical results match the expected results exactly. Figure A2 gives the time histories of the motion of the mass ( $q$ ,  $\dot{q}$  and  $\ddot{q}$ ) and frictional constraint forces acting on the mass when a sinusoidal displacement function ( $=\sin \omega t$ ) is applied to the end of the spring. The parameter  $D$  has a value of 0.6 when the block is stuck and 0.48 when the block is sliding. The forcing frequency is 67% of the natural frequency. The time histories indicate the expected stick-slip motion and are in general agreement with those obtained for a similar model using limit cycle solutions.

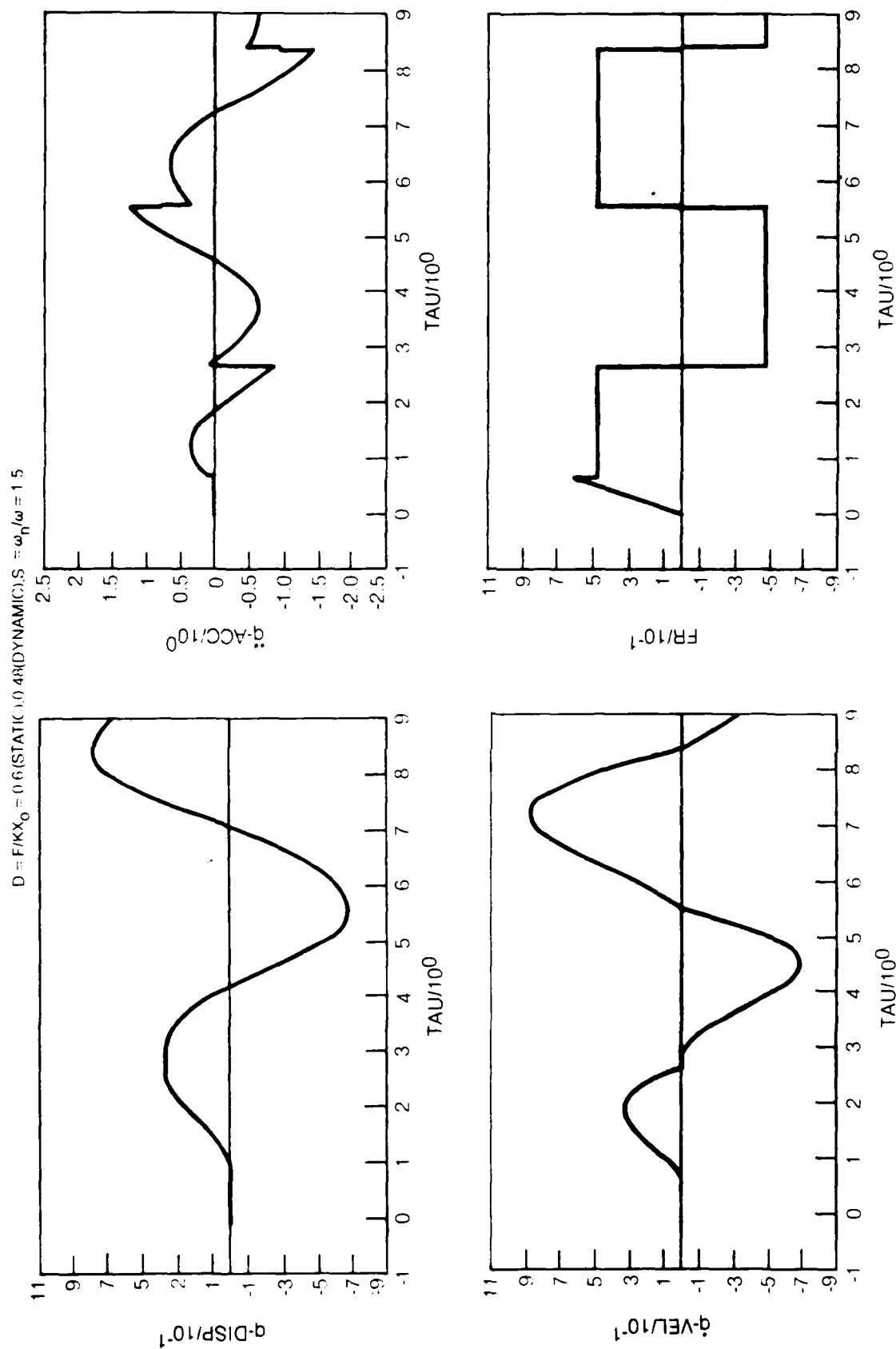


Figure A2. Single Degree of Freedom Coulomb Friction Model Motion ( $q, \dot{q}, \ddot{q}$ ) and Constraint Force (FR) Time Histories for Sinusoidal Spring End Displacement

## APPENDIX B

### APPLICATION OF FINITE ELEMENT CODES TO DRY FRICTION DAMPING

Five readily available finite element codes were reviewed for their ability to represent frictional forces. These included: ABAQUS (Ref. 30), ADINA (Ref. 31), ANSYS (Ref. 32), MARC (Ref. 33) and NASTRAN (Ref. 34). A concept commonly used in finite elements is to represent gap and friction effects as one dimensional (truss) nonlinear finite elements. A gap element would be represented by a spring connecting two nodes which has a very low stiffness when the nodes are separated and a high stiffness when the nodes are contacted. Figure B1 illustrates the concept. In Fig. B1, the gap is assumed to be open initially with a distance between nodes of  $\delta$ . The force in the spring is shown as a function of the relative displacement between the two nodes. If the initial gap distance  $\delta$  is negative, then the gap is initially closed. In a similar manner, the frictional force can also be represented. If Coulomb friction is assumed, the frictional force will be opposite to the relative displacements, but will be able to take on a maximum value given by the coefficient of friction times the normal load (the force in the gap element spring). Figure B2 summarizes the concept. Some computer codes consider the frictional force to be represented by a truss element which is elastic-perfectly plastic with a yield stress proportional to the gap force.

The ADINA manual written in 1977 did not contain any mention of provisions for describing friction, although this can be easily accomplished if not already completed. ABAQUS treats gap opening or closing and friction stick or slip as a boundary condition. ANSYS has a similar treatment. The gap and friction characteristics are input as elements but internally converted into appropriate boundary conditions. NASTRAN accounts for gap and friction effects with nonlinear elements. The MARC computer code previously considered the gap and friction characteristics to be represented by a special nonlinear element, but this was later abandoned because of inherent numerical instability.

Currently, the MARC code uses a LaGrange multiplier concept for the description of gap and friction effects. All of the above representations suffer from the fact that the opening and closing of gaps, and frictional stick or slip is highly nonlinear and contributes a great deal of numerical instability. Some of the frictional laws may be adapted for incorporating in the MARC code to determine: (1) their physical accuracy, (2) their numerical stability, and (3) their ease of use and implementation.



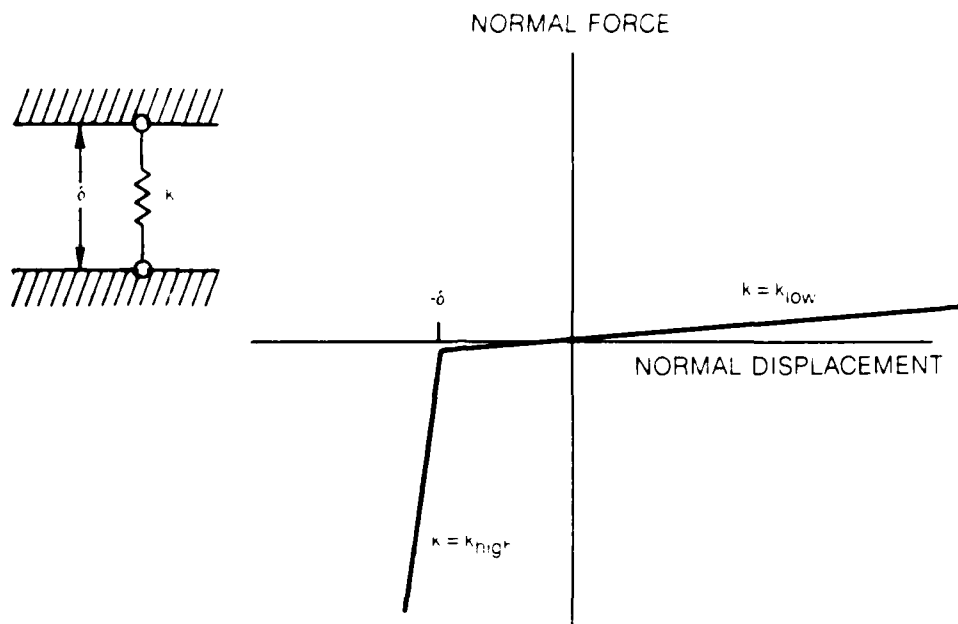


Figure B1 One-Dimensional Gap Element

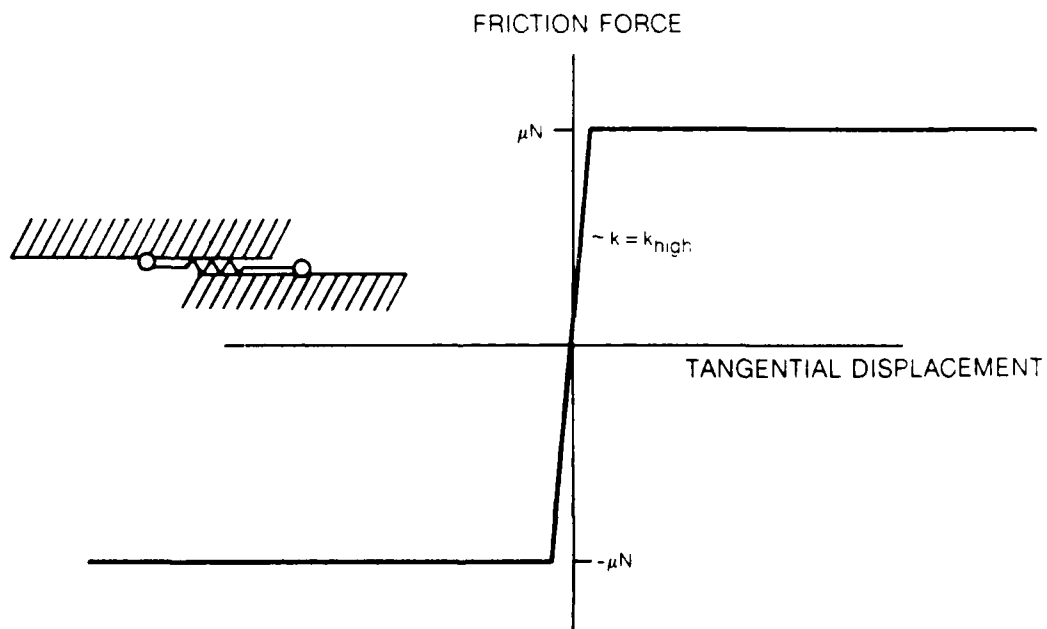


Figure B2 Two-Dimensional Friction Element

**END**

**FILMED**

---

**1-86**

**DTIC**